IEEE Access
Multidisciplinary | Rapid Review | Open Access Journal

Received November 14, 2019, accepted December 12, 2019, date of publication December 23, 2019,
date of current version January 7, 2020.

Digital Object Identifier 10.1109/ACCESS.2019.2961758

Linear Machines for Long Stroke Applications–A Review

IMANOL EGUREN[1], GAIZKA ALMANDOZ[1], (Member, IEEE), ARITZ EGEA[1], GAIZKA UGALDE[1], (Member, IEEE), AND ANA JULIA ESCALADA[2]
[1]Mondragon Unibertsitatea, 20500 Arrasate, Spain
[2]ORONA EIC, 20120 Gipuzkoa, Spain

Corresponding author: Imanol Eguren (iegurena@mondragon.edu)

The work of I. Eguren was supported in part by the Predoctoral Training Program of the Department of Education of the Basque Government.

ABSTRACT This document reviews the current state of the art in the linear machine technology. First, the recent advancements in linear induction, switched reluctance and permanent magnet machines are presented. The ladder slit secondary configuration is identified as an interesting configuration for linear induction machines. In the case of switched reluctance machines, the mutually-coupled configuration has been found to equate the thrust capability of conventional permanent magnet machines. The capabilities of the so called linear primary permanent magnet, viz. switched-flux, flux-reversal, doubly-salient and vernier machines are presented afterwards. A guide of different options to enhance several characteristics of linear machines is also listed. A qualitative comparison of the capabilities of linear primary permanent magnet machines is given later, where linear vernier and switched-flux machines are identified as the most interesting configurations for long stroke applications. In order to demonstrate the validity of the presented comparison, three machines are selected from the literature, and their capabilities are compared under the same conditions to a conventional linear permanent magnet machine. It is found that the flux-reversal machines suffer from a very poor power factor, whereas the thrust capability of both vernier and switched-flux machines is confirmed. However, the overload capability of these machines is found to be substantially lower than the one from the conventional machine. Finally, some different research topics are identified and suggested for each type of machine.

INDEX TERMS Linear machines, review, switched-flux, flux-reversal, doubly-salient, linear vernier, induction machine, switched-reluctance, power factor, magnet, demagnetization.

I. INTRODUCTION

Linear Machines (LMs) are electromechanical devices that, the same way as the Rotary Machines (RMs), convert electrical energy into mechanical energy and vice versa. Constructively, LMs are very similar to RMs. As described in Fig. 1, linear machines could be referred as rotary ones that have been cut out radially, and flattened so that the stator and the rotor lay horizontally facing each other [1].

Historically, linear motion has been generated based on RMs and rotary to linear conversion mechanisms, such as sheaves or gears. Nonetheless, LMs are capable of producing linear motion directly, without any kind of mechanical interface [2]. High acceleration and deceleration rates can be achieved with linear machines, as there is no possibility of slipping [2]. Railway transportation systems such as the JFK-New York AirTrain or the Linimo MAGLEV are a potential application for this type of machines [1].

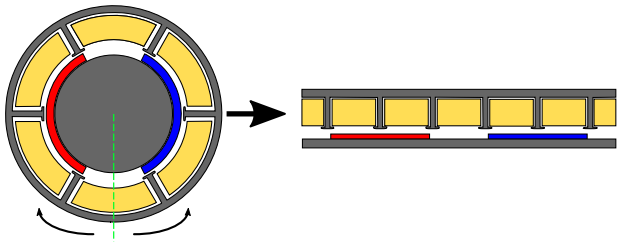

FIGURE 1. Transformation from rotary to linear machine.

The lack of gears allows linear drives a smooth operation, with reduced noise and vibration levels [3]. High precision

The associate editor coordinating the review of this manuscript and approving it for publication was Alfeu J. Sguarezi Filho.

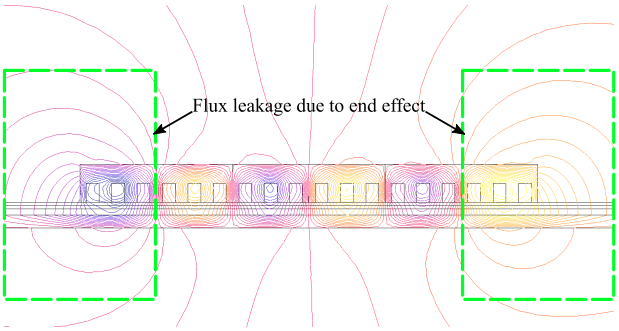

FIGURE 2. End effect of a linear machine.

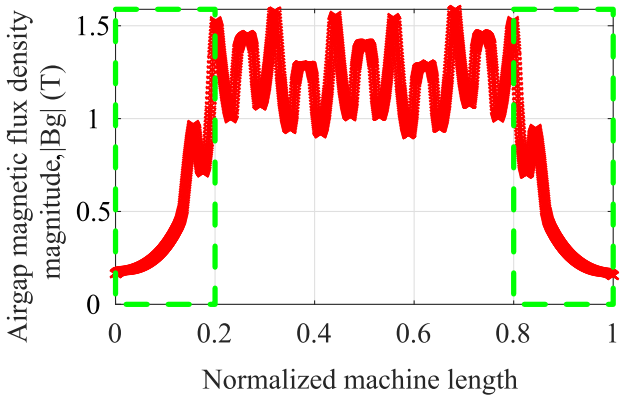

FIGURE 3. Magnetic flux density in the airgap of a linear machine.

and comfort are also possible with these machines, because as there are no gears, there is no backlash [4]. System-wise, the reduction of the amount of elements brings an enhancement of the reliability and the efficiency of linear motor driven systems [4], together with a lower maintenance requirement [5].

However, as the magnetic circuit has a start and an end in the edges of LMs, a new phenomenon called end effect appears in these machines (see Fig. 2 and Fig. 3). This effect produces some undesirable behaviours in linear motors, and that is why it has been subject of research for a long time [6]. It happens because the flux escapes from the ends of the machine, reducing the flux density in the air-gap of these regions. This generates an asymmetry between the central and external poles of a linear machine, which complicates the control and the analysis of LMs [7], [8]. Moreover, the end effect is also the reason why most of the linear motors have to deal with an unbalance between their phases [9], [10]. Due to the fact that there are only two ends in the machine, and 2 phases in 3 phase machines are wound through the end slots, one phase works at a higher flux density than the other two , generating the phase unbalance.

For every RM, there is a LM counterpart, so Linear Induction Machines (LIMs) [6]–[42], Linear Switched Reluctance Machines (LSRMs) [43]–[66], or Linear Permanent Magnet Synchronous Machines (LPMSMs) [67]–[93], can be found in the literature. Besides the different machine types, several topologies are described in the literature. Flat or tubular shapes, single-sided or dual-sided structures, modular configurations... there are many different options for selecting the ideal machine for each application.

In the last decade, a new and promising type of linear machine, Linear Primary Permanent Magnet Machine (LPPM), has emerged in the literature [3], [5], [22], [26], [74], [94]–[176]. However, a comprehensive review of linear machines for long stroke applications has not been published yet. The available review papers summarise the content from the literature, and do not verify those contents with a direct comparison of different machine technologies. Moreover, a direct comparison of the main types LPPMs and a LPMSM under the same operating conditions has not been found in the literature.

This paper first reviews the latest developments in linear machine technology. The capabilities and configurations of the different machine types are first presented. Then, based on the solutions found in the literature, some guidelines are listed to allow designers a fast configuration selection. A qualitative comparison of the main machine technologies is also given in terms of thrust density, shear stress, thrust per Permanent Magnet (PM) volume, thrust ripple and detent force, and PM immunity.

In order to validate the qualitative comparison, the most promising LPPMs are then selected and compared under the same dimensions and linear loading. It has been found that even if the literature review gives a precise enough prediction of the relative performance, there are several facts that must be taken into account when selecting a machine technology. When comparing the thrust of the selected machines, it is found that a poor overload capability may limit the applications of some of the machines with a high rated thrust density. The lower overload capability is also found to be one of the main drawbacks of all the LPPMs when compared to a conventional LPMSM. In addition, the PM immunity term is also divided into two parts, because the results demonstrate that some machines exhibit a poor PM working point at no load operation, even if the variation of the operating point of the PMs is low in fault conditions. Finally, the low power factor is identified as the other main drawback of all LPPMs when compared to a conventional LPMSM.

Sections II to V introduce the main machine technologies to date. Section VI summarises the different options to enhance a list of performances of linear machines. Section VII discusses the relative capabilities of the machines that have been found in the literature. The sizing and results of the selected machines are given in section VIII. Finally, in section IX the authors identify some of the remaining challenges and the most promising configurations for the selected machine technologies.

II. LINEAR INDUCTION MACHINES

Linear induction machines are one of the most common linear machine types nowadays. They are most widespread in railway transportation, where thanks to the non-adhesion

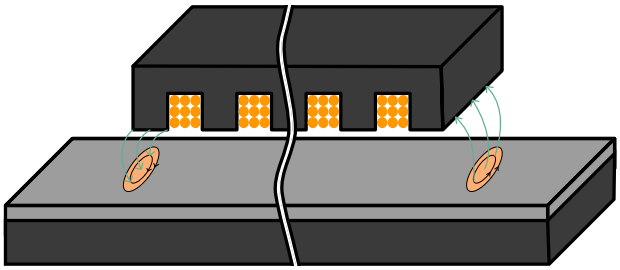

FIGURE 4. Dynamic end effect of a LIM.

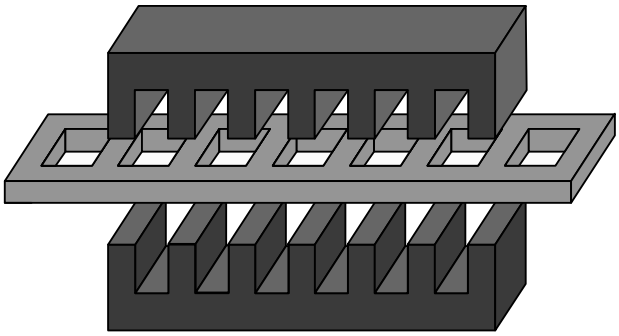

FIGURE 5. Double-sided ladder slit LIM.

thrust capability, LIMs allow climbing higher gradients than the conventional systems [21], [24], [26], [40]. Linear elevators and electromagnetic launch systems are also other applications where the implementation of LIMs has been studied [22], [41]. Their main advantages are their simplicity, robustness and low initial cost [22], [25], [26]. The absence of PMs also makes them inherently immune to irreversible PM demagnetisation, so their reliability is a remarkable feature [25].

However, much like in the case of rotary machines, the efficiency and power factor of LIMs still remain low [11], [26], [40], [42]. The losses of LIMs are even increased when compared to induction RMs due to the end effects, especially at high speed. When the drive is moving, new flux must be generated in the front side of LIMs. This induces eddy currents in the secondary that create an opposing magnetic field, which results in a braking force. A similar thing happens in the rear part of the machine, where the flux of LIMs should be vanished. Here, the reduction of flux generates eddy currents on the secondary that aim to maintain the flux at previous levels. Thus, an attractive force is generated in the rear part of the machine, which also contributes to the total braking force. This effect only happens when the machine is moving, and is known as dynamic end effect. It is obvious that, apart from the extra loss generated by the end eddy currents, thrust capability of LIMs is also reduced due to the dynamic end effect, because the machine has to deal with an inherent braking force [18], [34], [36].

There are three main fields where research is being focused for LIMs: Design [11]–[26], modelling [13], [15], [27]–[31] and control [9], [10], [32]–[40].

Regarding LIM design, there are three main secondary types that are being investigated. Sheet secondary LIMs are the most simple configuration [11], [13], [19]. A sheet secondary LIM is shown in Fig. 4. The secondary of these machines consists of a conductor sheet (typically aluminium) and the secondary back iron. The secondary of sheet LIMs gets even more simplified when adopting dual-side configuration, because the back iron is not needed anymore, thus consisting only of the conductive plate [22]. Despite their simplicity, sheet secondary configurations present an increased air gap length. The flux needs to get through the secondary sheet before entering the back iron, which reduces the flux linkage and thrust capacity of sheet secondary LIMs, as well as their power factor. In this sense, the performances of LIMs can be enhanced by employing a cage secondary [12] or a ladder-slit secondary [18], [19], [21], [25]. However, these secondary structures can negatively affect the thrust force ripple [18], and the complexity of the manufacturing process is also increased [19].

Different shapes of secondary cages are analysed and compared to a sheet secondary in [12]. Lee *et al*. conclude that the shape of the secondary can affect to the values of the equivalent circuit's parameters. When the thrust forces generated by a sheet secondary and different shaped cage secondary configurations are compared at rated slip, the results show that cage secondary type LIMs can generate higher thrust force. Besides, the phase currents are also reduced in the whole slip range. However, cage LIMs have to deal with a higher normal force.

A ladder slit secondary machine is designed in [19] for an urban rail transit application. The results show that both thrust and efficiency can be enhanced if the ladder structure is employed instead of the traditional sheet structure. Similar results are obtained in [21], where the transverse forces generated by sheet and ladder-slit secondary machines are also compared. The authors conclude that the ladder structure can help in laterally stabilizing and safely operating trains, because the transverse forces are mitigated. Reference [18] shows a design optimisation algorithm for ladder LIMs, based on a multiobjective multivariable optimisation technique.

Toroidal windings are also found to be much superior to conventional distributed windings in [17], when specified constraints include tight space requirements. Both thrust and efficiency are improved with this type of windings. Nonetheless, the toroidal winding must be manufactured by hand, thus, the manufacturing process gets more complicated this way.

Optimisation techniques have also been proofed to be useful in the design of sheet secondary LIMs. In [13] the authors select particle swarm optimization method, as the search algorithm for the optimal design. A combination of optimal Latin-hypercube design and progressive quadratic response surface methodology is employed to optimise a single-sided LIM in [14].

The optimisation of the efficiency has also been assessed control-wise. An integrated inverter and LIM loss model is proposed in [40]. Hu et al. reduce the losses of the system

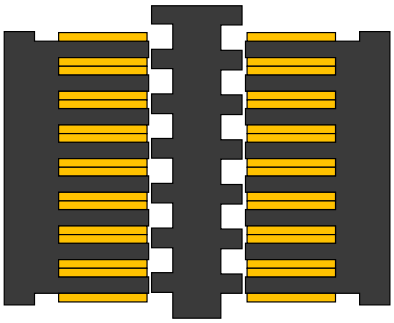

FIGURE 6. Four phase linear switched reluctance machine.

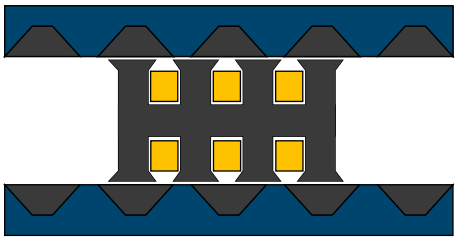

FIGURE 7. Segmented secondary LSRM.

by 3-4 %, which can reduce the energy consumption significantly in linear metro systems. The control has also been used to compensate the influence of the end effect [35], [36]. A combined vector and direct thrust control is proposed in [38]. The experiments show that the proposed control can operate a LIM smoother than the direct thrust control, and the dynamic performance of the conventional vector control is improved with the new solution.

Modelling of LIMs is another important field for both design and control perspectives. The search for a precise but simple enough equivalent circuit as the one for induction RMs has been assessed in many research papers [13], [15], [27]–[31]. Duncan's is a well known equivalent circuit. It assumes an exponential increase of the air gap flux density, and proposes a simple function for analysing the end effect in the T-model induction RM equivalent circuit. Based also in the T model, Xu et al. [28] propose an equivalent circuit that by four relative coefficients takes account of both end and edge effects. The equivalent circuit is also given in dq and $\alpha\beta$ frames.

In spite of all the research that has been developed around LIMs, their efficiency, power factor, and dynamic braking force make them unsuitable for many applications.

III. LINEAR SWITCHED RELUCTANCE MACHINES

Feature-wise, linear switched reluctance machines (LSRMs) are very similar to LIMs. Their main advantages are their low material and manufacturing cost [53]–[55], simple structure [57], [64], [66], and their inherent ruggedness [61], [64]–[66].

They consist of a toothed structure on both primary and secondary sides, and do not require permanent magnets or windings in the secondary as it can be seen in Fig. 6. The low number of elements makes these machines very easy to manufacture [60], [63], and their wide constant power operating range [53], [58], has made them an interesting candidate for their application in elevators [43], [57], [65] or rail transit applications [53].

These machines generally rely on the variation of self-inductance to generate thrust force, and exhibit very low mutual-inductance values. This makes them highly reliable and fault tolerant [44], [46], [57], [59]. They are also capable of achieving higher thrust densities than LIMs [53], [59], while lowering thermal management requirements on their secondary side [48], [49]. Even so, their thrust capability is still lower than the one from LPMSMs [51], [65], [127].

Thrust ripple, and high noise and vibration levels are common issues when these machines are used [58], [65], [66]. A common approach for reducing issues with the generated thrust ripple is the usage of the so called force distribution functions, which reduce the output force ripple by controlling the waveforms of the input currents [49]. However, apart from the reduction of the thrust force ripple, this control solution also reduces the average thrust produced by LSRMs, so the designer has to decide between higher ripple or lowered thrust density values.

In the last years, two new topologies of LSRMs are showing promising performance improvements. These are the segmented secondary LSRMs [51], [53], [57], [59], [61] and the mutually coupled LSRMs [50], [52], [55], [58], [60].

By adopting a segmented structure, LSRMs have been found to improve the thrust density, while lowering the machine cost [57], [61], thanks to the suppression of the yoke in the secondary side. These machines can be configured with a secondary pole width to secondary pitch ratio of almost 1, much higher than the 0.5 limit for the conventional tooth type LSRMs. This means that the segmented configurations can carry more flux, and thus increase power density when compared with tooth type LSRMs [57]. A complete guide for designing segmental secondary LSRMs is given in [61].

Mutually coupled LSRMs have not received that much attention yet. Some papers have been published [45], [60] analysing these configuration in the linear form, but most of the current research refers to rotary switched reluctance machines [50], [52], [55], [58]. It is found that due to the double phase excitation capability of mutually coupled switched reluctance machines, their efficiency and power density values are higher than the ones from conventional machines. Kabir and Husain [52] conclude that the performance of this type of machines is comparable to that of the Toyota Prius interior PM machine in terms of torque density, efficiency and operating range. Lower noise and vibration levels are reported for these machines in [50], due to much lower radial forces than in classical switched reluctance motors. In the linear form, a mutually coupled LSRM has been compared to a LPMSM in [60], and the results show that for machines of the same dimensions, the mutually coupled LSRM can produce 1.6 % higher electrical power at rated velocity, while reducing the cost of the machine by 62 %. In spite of all

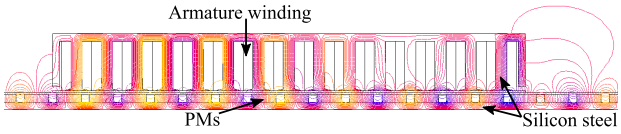

FIGURE 8. End effect of LPMSMs.

of these advantages, mutually coupled switched reluctance machines are not as fault tolerant as the conventional counterparts, because they use the mutual flux to generate thrust. Moreover, a distributed winding is required for this type of machines, and thus, the end windings are bulkier, and may result problematic when tight space requirements are set [52].

IV. LINEAR PERMANENT MAGNET MACHINES

In the same way as in permanent magnet RMs, LPMSMs show an excellent thrust force density, efficiency, power factor and controllability [83], [85], [89]. Their advantages make them a strong candidate for applications such as ropeless elevators [76], [80], [177], factory automation [78] and high precision machine tooling [177]–[179].

However, LPMSMs are also affected by the end effect. Apart from the previously cited phase unbalance and flux density reduction, the end effect is also source of an additional thrust force ripple component known as end force or end effect force in LPMSMs. This force affects them even at no load condition [75], [90], [93].

Depending on the relative position between the primary and the secondary parts, the magnets on one side or another will attract the machine ends with more strength, generating the end effect ripple. The no load thrust ripple, also known as detent force, is the result of the sum of the conventional slot effect or cogging force and the end effect force [90], [93], [179]. As LPMSMs have to deal with multiple detent force ripple sources, several different solutions have been tested in order to reduce the open-circuit thrust pulsation, e. g. skewing magnets, adjusting the primary length, and slot shifting [69], [81], [85], [93].

A comprehensive analysis of the performance of a LPMSM with different step-skew configurations is reported in [81]. Cai *et al*. mention that the optimal skew angle to suppress the cogging is different from the optimal angle to suppress the end force. The orders of end force harmonics are low, an thus, suppressing those via the skew would also lower the average thrust force.

A two dimensional detent force reduction method is showed in [85]. The authors achieve a reduction of 94 % in the detent force ripple by employing two different primary lengths to suppress the end force and a slot-shift method to deal with the slot effect.

The performance of a segment-shifted machine can be improved with a rearrangement of the windings [90], [92], [93]. As the average thrust force is reduced with the increase of phase or pole shifting distance, the authors suggest that rearranging the winding configuration in the different primary sides can be a good solution for reducing the detent force without losing any force production capability.

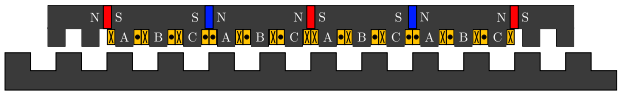

FIGURE 9. Linear doubly-salient machine.

Modern optimisation techniques have also been applied to LPMSMs. A genetic algorithm is employed to optimise an air-core LPMSM via different objective function configurations in [70], [71]. The results clearly improve the performance of the original motor. A combination of Taguchi method and Finite Element Method (FEM) is employed in [86]. The authors compare the resultant machine with the optimal machine obtained from the optimisation via an analytical model and particle swarm optimisation. The results show that the combination of Taguchi method with FEM can produce better results than the previous optimisation method.

Due to the high cost of PM materials, the material cost of LPMSMs can be prohibitive in long stroke applications [78]. In the last decades, a new family of linear PM machines, known as flux-switching machines [3], [5], [22], [26], [74], [94]–[139], [139]–[146], and primary PM Vernier machines [147]–[176] are drawing much attention. All these machines consist of an active primary that contains both windings and magnets, and a passive secondary with no PMs or copper, similar to that of LSRMs. Although these machines are still a type of LPMSM, they are grouped in a different section in this document.

V. LINEAR PRIMARY PERMANENT MAGNET MACHINES

There are four main types of LPPMs currently in the literature. These machines are Linear Switched-Flux Permanent Magnet Machines (LSFPMs) [3], [5], [22], [26], [74], [94]–[127], [139], Linear Flux-Reversal Permanent Magnet Machines (LFRPMs) [128]–[144], Linear Doubly-Salient Permanent Magnet Machines (LDSPMs) [145], [146] and Linear Vernier Permanent Magnet Machines (LVPMs) [147]–[176]. Their structural advantage over conventional LPMSMs, i.e., the absence of PMs in the secondary, has brought a huge amount of research involving these LPPMs. In this section, their working principles and the latest research related to them are presented.

A. DOUBLY-SALIENT MACHINES

Doubly-salient machines, are commonly grouped within the flux-switching machine family, together with LSFPMs and LFRPMs. All these share a similar topology and working principle, but there are some slight differences in both their operation and performance aspects. Doubly-salient machines are an already very mature technology [180]. They consist of a primary with a concentrated winding and PMs inserted in the primary yoke, and a doubly-salient passive secondary. Figure 9 shows one of the machines presented in [145].

Overall, the LDSPMs exhibit a great PM immunity and robustness [145], [146], [180], [181]. Together with the high thrust density and efficiency achieved thanks to PM

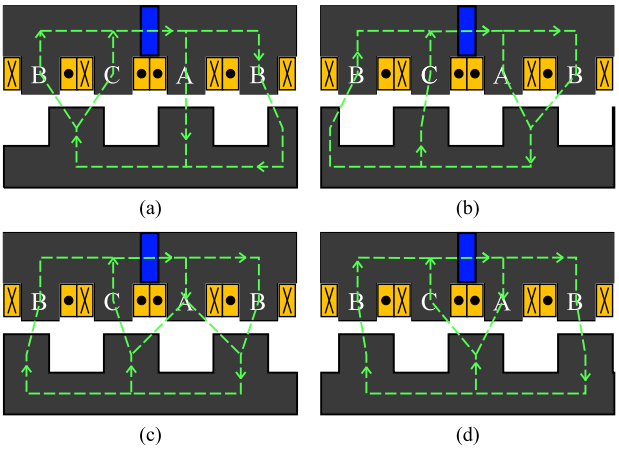

FIGURE 10. No load flux paths of LDSPMs. (a) Initial, (b) 90 degree, (c) 180 degree and (d) 270 degree.

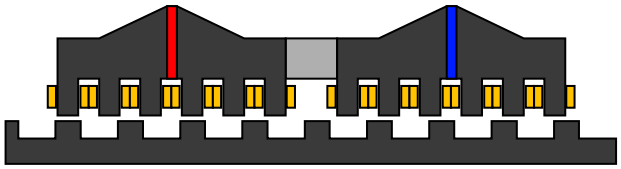

FIGURE 11. Modular and complementary LDSPM.

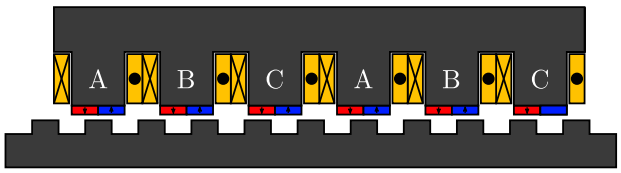

FIGURE 12. Linear flux-reversal machine.

material, LDSPMs offer really interesting capabilities for applications where high reliability is the main requirement. Regarding manufacturing costs, LDSPMs require the lowest amount of PM volume between flux-switching machines for a given average thrust value [181]. Besides material cost, LDSPMs are also easily manufactured [181], which is also another important benefit of these machines. In general, these machines generate a trapezoidal waveform of the back-EMF. Thus, they are naturally suited for a Brushless DC (BLDC) control operation [145], [146].

Nonetheless, the performance of LDSPMs is strongly affected by the detent force and on load thrust force ripple [145], [146]. Moreover, the unipolar nature of the flux in LDSPMs is a known issue [106], [137], [145], [181]. Notice how the flux linked by a coil in Fig. 10 keeps a constant direction over a full period. This reduces the force capability of these machines [106], [180]. However, LDSPMs are still an interesting solution for long stroke applications, and their usage in applications such as urban rail transit has already been proposed in some research papers [145], [146].

Not many publications involving LDSPMs have been found in the literature. In [145], Cao *et al.* compare the conventional structure of LDSPMs with a modular and complementary one. The authors achieve a noteworthy reduction in the thrust force ripple and the detent force ripple with the new structure, from 40 % and 35.7 % to 8.6 % and 12.15 % respectively. Moreover, the average thrust per PM volume and shear stress are also improved with the new configuration from 5.5 MN/m^3 and 8.39 kN/m^2 to 6.94 MN/m^3 and 10.72 kN/m^2 respectively. The authors also analyse both the BLDC and the Brushless AC (BLAC) (with $I_d = 0$) operating modes of the machines, and the results show that a slightly larger thrust and a lower ripple can be generated when the machines are driven in BLAC mode.

The same authors propose the usage of the conventional LDSPM for an urban rail transit application. Cao *et al.* first discuss the best end teeth configuration to reduce the detent force of the machine. Different skew angles are discussed later on, to reduce the remaining ripple of the machine. In this case, the proposed LDSPM achieves lower thrust density and shear stress values with 66 kN/m^3 and 5.12 kN/m^2 respectively, which are rather low for PM excited machines. The authors propose the usage of a BLDC operation for the unskewed configuration, and a BLAC operation with all the current injected to the q-axis when a skew is applied to the machines.

B. FLUX-REVERSAL MACHINES

Linear flux-reversal machines, much like all the machines in the flux-switching family, are well known thanks to their high efficiency, thrust density and robustness [132]–[136], [138], [140], [141], [180], [181]. In the case of LFRPMs, two PMs are mounted on the surface of each primary teeth with alternated magnetisation, as shown in Fig. 12. Due to their placement, the flux from magnets is in series with the flux generated by the armature winding. Thus, these machines suffer from poor demagnetisation immunity under fault conditions [137], [143].

The operating principle of these machines is similar to the LDSPMs. Nevertheless, LFRPMs are able to link bipolar flux in their primary coils. Notice how the sense of the flux is reversed when the secondary tooth in Fig. 13 moves from one magnet to the adjacent one. So, higher thrust density values should be expected from LFRPMs when compared to LDSPMs. In this case, the natural back-EMF waveform of these machines is sinusoidal, thus, they are most suited to be driven in a BLAC operation [129], [137], [138]. The *dq* frame inductances of these machines generally display similar values, thus, the best option is to control them with the direct current, I_d, set to 0 [133], [137], [138].

In the seek of performance improvements, several different solutions can be found in the literature. Due to the existing concerns around the price of rare-earth materials [182], reduction of PM material is one of the main research fields concerning LFRPMs. In [129] the authors propose a consequent-pole configuration to achieve a 50 % reduction of the volume of PMs used in the machine. Moreover,

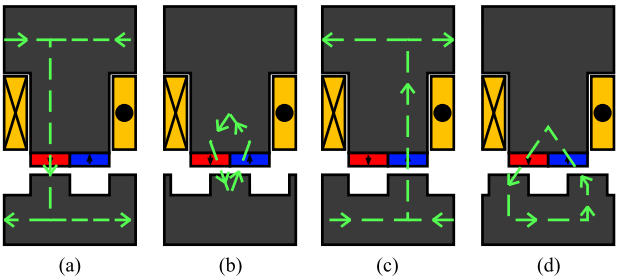

FIGURE 13. No load flux paths of LFRPMs. (a) Initial, (b) 90 degree, (c) 180 degree and (d) 270 degree.

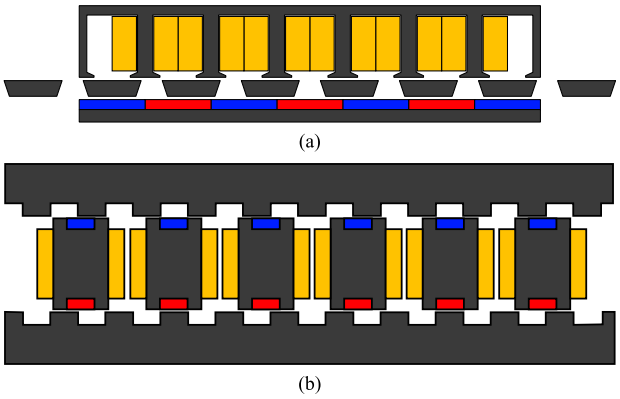

FIGURE 14. (a) Partitioned-stator LFRPM and (b) Consequent-pole and yokeless LFRPM.

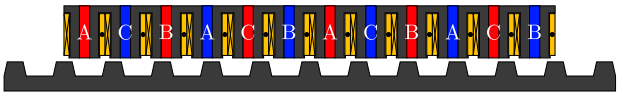

FIGURE 15. 12/10 pole linear switched-flux machine.

the thrust capability with the consequent-pole configuration is also 22 % higher than the one from the original machine. Combining the consequent-pole topology with a yokeless structure, Gandhi *et al*. increase the average thrust force of the conventional LFRPM machine in 33 % [130]. A greater reduction of PM volume is achieved in [141] by adopting the consequent-pole structure and suppressing half of the primary teeth. Shi *et al*. [141] manage to achieve an improvement of 51 % of the average thrust while reducing 75 % of the PM usage volume with a large slot-opening LFRPM. Nevertheless, a more comprehensive research of this machine topology is needed, because it has not been found anywhere else in the literature.

Improvement of the fault-tolerant capability is another area that has drawn attention of researchers. A LFRPM with a modular and complementary magnetic circuit is proposed in [131]. Thanks to the adopted structure, the resulting machine achieves a high fault-tolerant capability as the ratio between the mutual-inductance and the self-inductance is reduced to 4.6 %. Besides, a thrust ripple of 10.2 % and a detent force of 5.4 % are achieved by the proposed machine. A similar phase decoupling is also obtained in [132] thanks to the insertion of fault-tolerant teeth. However, the flux linkage of the machine in [132] is unipolar [134], so Xu *et al*. employ another modular an complementary structure to reduce the aforementioned ratio to a 4.5 %, while improving the thrust density of the fault-tolerant LSFPM machine from 113.7 kN/m^3 to 158 kN/m^3 [134].

The improvement of thrust density is also researched in the literature. Shuraiji, Zhu *et al*. [133], [138]–[140] employ a partitioned-primary structure to improve the thrust density of conventional LFRPMs. For machines with same dimensions and current density, a remarkable improvement of 118.9 % is reported in [138]. The authors also mention that due to the partitioned-primary structure, the PM immunity is also improved, as the flux from the primary coils is not directly applied to the magnets. Transverse-flux LFRPMs are also proposed in the literature in order to improve the thrust density of these machines [135], [137], [142]–[144]. A comprehensive analysis of a transverse-flux LFRPM is published in [137]. The presented machine can produce a thrust density of 153.5 kN/m^3 and a shear stress of 8.4 kN/m^2, but both the detent force, 22 % and the thrust ripple, 34.4 % are high for the proposed LFRPM. It is a known issue that transverse-flux machines require 3D FEM simulations to analyse their performance. In this aspect, Dong *et al*. [142] propose a 2D FEM equivalent model for the analysis of a transverse-flux LFRPM. The measurements obtained with a prototype show a good agreement between predicted and measured values.

Although it is not mentioned in the literature for machines with a linear form, rotary flux reversal machines generally suffer from low power factor [78], [183]. This is a characteristic that should be improved in order to enhance the feasibility of LFRPM drives.

C. SWITCHED-FLUX MACHINES

The other machines in the flux-switching family are the switched-flux machines. In fact, they are the machines that can produce the highest thrust density in the flux-switching family [114]. The primary of conventional LSFPMs consists of U-shaped silicon-steel modules joined by PMs of alternate magnetisation, so that each magnet is sandwiched between two modules and a concentrated winding. Figure 15 shows a conventional 12/10 primary/secondary pole machine. The LSFPMs produce highly sinusoidal back-EMF waveforms, and thus, they are most suited for a BLAC operation [3], [119], [121], [125]. The reluctance force in this case is generally negligible too, thus, the sinusoidal phase currents are generally supplied in phase with the back-EMFs for an optimum operation [3], [119], [121], [125].

In this case, the magnetisation direction of PMs is perpendicular to the flux generated by the primary coils. This provides LSFPMs a great immunity against demagnetisation in case of faults in the primary winding [5], [74], [108], [124]. The immunity of PMs against permanent demagnetisation enhances the capability of LSFPMs work in the flux-weakening area [95], [104], [106]. A good overload

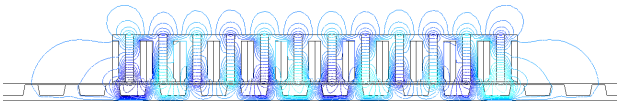

FIGURE 16. Open circuit flux-lines of a 12/10 LSFPM.

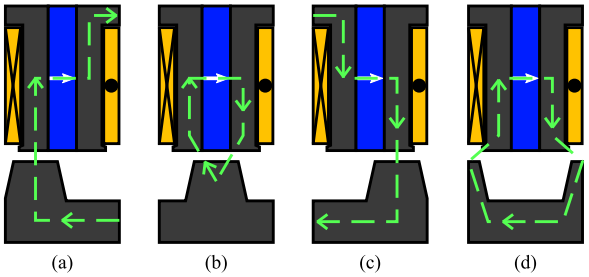

FIGURE 17. No load flux paths of LSFPMs. (a) Initial, (b) 90 degree, (c) 180 degree and (d) 270 degree.

ability is also mentioned in [5], [96], [108] for the same reason.

One of the main drawbacks of LSFPMs is the reduced space of the primary side. The designers have to deal with limited magnetic loading and slot areas [104], [106], [107], [139]. Moreover, due to the modular structure, the primary of LSFPMs tends to be mechanically weak [102], and their detent and thrust ripple performance is quite sensitive to manufacturing tolerances [102]. In fact, both the no load and on load ripples of LSFPMs are generally quite high [3], [26], [98], [113], [127]. Another drawback of LSFPMs is the amount of PM material that they require per unit of thrust [74], [103], [104], [106]. Due to the primary structure, the uppermost area of the magnets suffers from a severe flux leakage problem as it can be seen in Fig. 16.

There is yet another drawback for LSFPMs when compared to conventional LPMSMs. As the secondary does not have any magnets, the flux is bipolar in this side too. This means that iron loss is also present in this side, thus lowering the efficiency of LSFPMs [100], [118].

However, the iron losses can be used as a safety feature. In [118], Zhang *et al*. propose a LSFPM with a non-laminated secondary for a low-speed elevator. With their solution, the authors limit the falling speed to 1.35 m/s without any other safety devices. The usage of LSFPMs for elevators is also analysed in [114], [120], [121]. LSFPMs have also been applied for rail transit [26], [124], [184] and electromagnetic launch systems [22], [125].

One of the most researched fields for LSFPMs is their thrust ripple. Skewing the secondary was classified as ineffective in [98]. In [101] Wang *et al*. propose to use two additional teeth in each end of the primary to reduce the end effect component of the detent force, and to apply the skew to lower the amplitude of the remaining harmonics afterwards. Additional PMs are placed in the ends of the machine in [105]. The aim of this solution is to balance the back EMF waveforms of the three phases of the machine, so that the electromagnetic thrust ripple is lowered. This solution is also tested in [114]. In this case, the on-load thrust ripple is 16.6 % lower after balancing the EMFs. Nonetheless, the addition of end PMs enlarges the detent force to 1.96 times the initial value. To reduce the detent force when employing additional PMs, a combination of those with additional assistant teeth can be employed [121]. Complementary solutions have also been employed in LSFPMs. Cao *et al*. [184] use a modular and complementary structure to reduce the ripple of the machine. Due to the complementary structure, the amplitude of the even harmonics of the back-EMFs is reduced to an almost negligible value. This reduces the ripple of the electromagnetic thrust. Moreover, due to the displacement between different modules, the detent force is also lower than the one from the original machine. A combination between end PMs and a complementary magnetic circuit is proposed in [3]. The authors compare a LSFPM with a sandwiched LSFPM, and results show that even if the thrust ripple is reduced in both cases, the sandwiched LSFPM shows the lower thrust ripple.

Fault-tolerant capability is also obtained in by employing a modular structure [103], [113], [184]. In such modular structures each module only contains one coil, so the phase unbalance can be neglected, as all the individual modules are affected by the end effect in a similar order of magnitude. A parameter sensitivity analysis is performed in [113] for modular and complementary machines. By removing the PM from half of the primary teeth, E-Core LSFPMs improve the fault-tolerant capability of conventional LSFPMs without sacrificing average thrust production [107].

In order to improve the thrust density of LSFPMs, C-Core LSFPMs are proposed in [107]. Compared to the conventional 12/10 LSFPM, the 6/13 C-Core machine can achieve a 18.4 % higher average thrust force while the amount of PM material is 40.1 % lower. However, the detent force is increased from 10.39 % to 13.32 %. Besides, the power factor is generally low for C-Core LSFPMs [106]. A yokeless C-Core LSFPM is presented in [5]. The particularity of this design is that it adopts a series magnetic circuit, and doing so, Gandhi *et al*. improve both the thrust density and the power factor of a conventional LSFPM, 56 % and from 0.168 to 0.6 respectively. The proposed machine also reduces the average normal force value to zero. A similar structure is proposed in [125] and [22], by adopting a double mover structure with a series magnetic circuit. However, the proposed machine has a long primary configuration, so the performance is very poor from both efficiency and power-factor viewpoints. The partitioned-stator configuration has also been proposed for LSFPMs, and an improvement of 32.2 % on the average thrust force has been reported [119].

D. VERNIER MACHINES

Linear vernier machines employ the so-called magnetic-gearing effect to produce high thrust force and to work at low speed [154]. LVPMs can be configured with the PMs on either the primary [154], [172] or the secondary side [164], [167]. For long stroke applications, the cost of the secondary PM

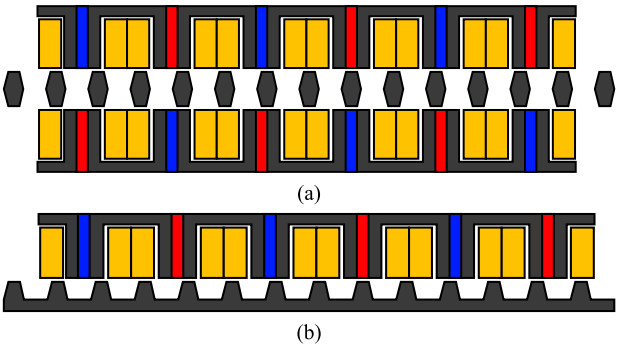

FIGURE 18. (a) Double-mover C-Core LSFPM with series magnetic circuit and (b) single sided C-Core LSFPM.

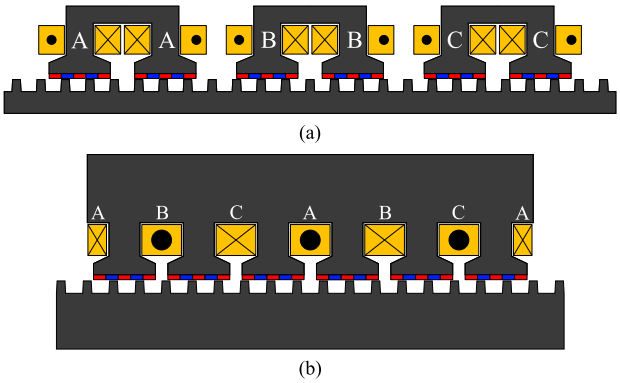

FIGURE 19. (a) Linear vernier hybrid machine and (b) linear primary permanent magnet machine.

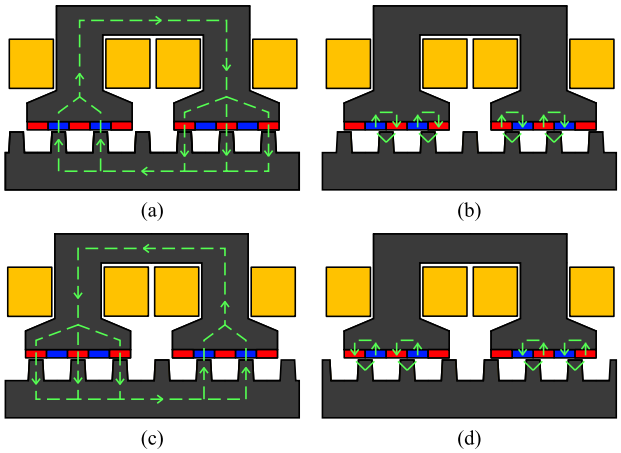

FIGURE 20. Flux paths of LVHs. (a) Initial, (b) 90 degree, (c) 180 degree and (d) 270 degree.

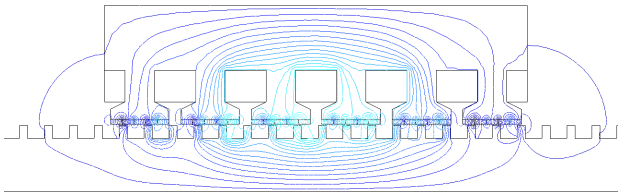

FIGURE 21. Open circuit flux-lines of a LPPMV.

LVPM is excessive, so it has been left out of the scope of this review.

Generally, LVPMs show excellent shear-stress values and a high thrust density [147]–[154]. In addition, these machines exhibit high efficiency values even at low speed, thanks to the aforementioned magnetic gear effect [158]. Furthermore, very low thrust ripple values can also be achieved with LVPMs [158], [160], [167], [176]. Contrary to other machines, LVPMs can achieve low speeds and still maintain a reasonable size and number of primary slots [157], [168], [172], which simplifies its structure.

Much like LFRPMs, LVPMs have the PMs mounted on the surface of the primary teeth, but the amount of PMs is larger in order to increase the rate of change of the flux and achieve higher back-EMF values [153]. Two main topologies of LVPMs have been found in the literature: Linear Vernier Hybrid Machines (LVHMs) and Linear Primary Permanent Magnet Vernier Machines (LPPMVMs).

For the former type, the operating principle is quite similar to that of LFRPMs. The flux is reversed when the secondary poles are displaced from one primary magnet to the adjacent one. The only difference is that there are more poles and magnets in LVHMs. Thus, the relative displacement between the mover and the stator needs to be much lower for the flux to fulfil an entire period, as it can be observed in Fig. 20. The main difference between LVHMs and LPPMVMs is that the modulation of the airgap flux is done progressively in LPPMVMs. In these machines, the secondary teeth modulate the flux density from the magnets so that the primary core perceives a lower amount of poles, to work at a higher frequency. The modulation effect is displayed in Fig. 21. The effective pole pair number in the primary p_{ef}, travelling speed of the flux in the primary core v_{ef} and gear-ratio G_r of LPPMVMs can be calculated with:

$$p_{ef} = |p_{PM} - n_t| \tag{1}$$

$$G_r = \frac{n_t}{n_t - p_{PM}} \tag{2}$$

$$v_{ef} = G_r \cdot v_m \tag{3}$$

where p_{PM}, n_t and v_m stand for PM pole pair number, number of secondary teeth and mechanical speed.

If analysed closely, it can be seen in Fig. 19 that the alignment between the primary magnets and the secondary poles is constant within a primary tooth for LVHMs. In contrast, this alignment is not kept constant in LPPMVMs. This is the main reason why LVHM machines suffer from a higher cogging force [152], [154] than LPPMVMs. In fact, the cogging force of LPPMVMs is usually very low [151], [152], [154].

Even if their structures are slightly different, both of these machines are usually controlled in the BLAC mode, with the sinusoidal currents injected in phase with the back-EMFs [156], [172], [175].

LPPMVMs adopt overlapping distributed windings for their primary armature, in order to maximize the gear ratio [154]. On the other hand, LVHM machines employ

concentrated windings. This results in a thicker yoke and bulky end windings for LPPMVMs, and thus, LVHMs exhibit a higher thrust density [154]. In addition, LVHMs adopt a modular structure most of the times [147], [148], [154], [161], so their performance is less affected by the end effect [154]. A detailed comparison between these two machines is done in [154].

For variable speed drives, it was shown that vernier machines have a very narrow constant thrust speed range [158]. The performance at the constant power speed range is not good either for this machines, as the operating efficiency is low when compared to an Interior Permanent Magnet (IPM) machine [158]. However, the main drawback for all LVPMs is their low power factor [168]–[176]. This means that LVPMs require costly inverters that can manage high currents if phase voltage is fixed.

That is the reason why power factor improvement has received much attention in the last years. Baker *et al*. compare different PM configurations for a consequent-pole LVHM in [169]. The authors conclude that the most effective topology is the V-shape IPM. With such solution, the power factor is improved from 0.45 to 0.67. The optimal shape of PMs for the same type of machine is discussed in [172]. Another consequent pole structure is proposed in [157] to reduce the volume of PMs. Not only does the proposed machine reduce 25 % of the PM volume, but also the thrust capability of the consequent pole machine is 34 % higher than the one from the original machine. Thrust capabilities of a conventional LVHM and a consequent-pole LVHM are also compared in [161]. In this case, an improvement of 14.3 % is obtained in the thrust density, and the PM volume is 50 % lower. The usage of halbach arrays is proposed in [153] for an artificial heart machine, in order to improve the usage of PMs. The proposed configuration can generate higher thrust force and lower detent force than the conventional LVPM.

A high power factor LVPM can be designed by combining a double-sided structure and a series magnetic circuit [155], [170], [171] (Fig. 22). The design parameters of the machine in [171] are globally optimised for maximising thrust and power factor. The final design achieves a power factor of 0.945, but the experimental measurements of thrust differ from the expected values in up to 17.2 %, and the value of the power factor is not verified with the prototype. Further research must be done in order to validate this solution. Another double-sided LPPMVM with a series magnetic circuit is proposed in [156]. The power factor is not directly analysed, but the proposed machine exhibits 45 % lower inductance values, so an improvement in the power factor should be expected. Moreover, the presented machine improves the thrust density and shear stress of the previous machine, from 283 kN/m^3 and 44.4 kN/m^2 to 387 kN/m^3 and 49.4 kN/m^2.

VI. GUIDELINES FOR PERFORMANCE ENHANCEMENT

Several different configurations have been found in the literature in the seek of improving the characteristics of LPPMs.

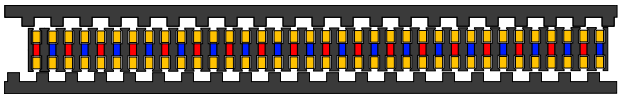

FIGURE 22. High power factor LVPM.

In this section, several desired features are listed and the solutions that have been detected in the literature for each feature are described. LIMs are left out of the scope of this analysis, because their main drawback, namely the dynamic end effect, has to be dealt with inherently.

A. THRUST FORCE DENSITY

To start with, the thrust force density is one of the most important characteristics of LMs. In general, gears and pulleys are removed for linear motor driven systems. Consequently, requirements many times involve low speed and high thrust capabilities. Thus, in order to reduce the bulk and material cost of LMs, the thrust density must be maximised.

Consequent-pole machines (Fig. 14 (b)) are capable of improving the thrust density of LPMSMs [129], [142], [157], [161], [162]. This is achieved because, due to their structure the flux leakage is reduced [157], [161], [162], [174].

Halbach arrays can improve the usage of PMs by concentrating the flux density in one side of the arrays [163], [174], [176], [186]. Moreover, as the flux generated by the magnets is almost completely shielded to a single side, very small yokes or even non-magnetic materials can be used with such configuration [187].

Thanks to the flux-focusing effect IPM configurations can enlarge the flux density in the airgap, which results in an increased thrust density [164], [168], [169], [172], [176].

Double-sided machines generally exhibit a higher thrust capability than the single-sided counterparts [16], [47], [84], [85], [92], [93], [124], [138]. In such machines, the yokeless structure can enhance the thrust density of the conventional configuration [5], [120], [156]. By removing the primary or secondary yoke, the height of the machines, and thus the cost in long rail applications, can be significantly reduced. Partitioned-stator configurations (Fig. 14 (a)) have been demonstrated to enhance the thrust density of LMs [119], [138]–[140], [185]. In primary PM LMs only LSFPMs and LFRPMs partitioned-stator machines have been found in the literature. Both doubly-salient and vernier machines could also benefit of this structure.

More so, by combining some of the previous solutions, the enhancement of the thrust density can be improved even more, e. g. a halbach-array partitioned-stator LFRPM machine could improve the thrust density of the machine in [138], by reducing the size of the second primary yoke.

B. THRUST FORCE RIPPLE

There are two main sources of thrust force ripple in LPMSMs, i.e. detent force and phase unbalance. The detent force also consists of two components: end effect force and traditional cogging force.

If the main requirement of the installation is the removal of force ripples, air-cored machines are a great solution, as they are not affected by any means by the detent force [70], [71], [76]. However, the thrust density of these machines is quite low [70], [71], [76], [82], [188], and either armature windings or secondary magnets need to be mounted in the long rail. Thus, core-less designs result in high-bulk and high-cost machines. Even so, these machines can be interesting candidates for ultra-high precision applications.

The usage of assistant teeth is a common solution for dealing with the end-effect force [101], [107], [121]. However, this solution implies an increased active length the machine, so if that dimension is strictly limited, other solutions must be found. Complementary configurations are another effective solution. As the complementary modules are displaced 180°, all the odd harmonics of the detent force are in counter-phase, and thus, they compensate each other [109], [118], [123], [184]. Moreover, this solution also suppresses even order harmonics of the back-EMF. So it is also an effective solution to reduce the electromagnetic thrust ripple. Modular solutions are another option [184] if an adequate module-displacement is selected, both the detent force and phase voltage unbalance can be almost completely compensated.

Segment-shifting [85], [90], [93] has also been proven to be effective in the reduction of the end-effect force. Moreover, if the windings are rearranged, the reduction of the EMF can be compensated [90], [93].

Finally, by attaching additional magnets at the ends of the machine, the unbalance of the back-EMF can be completely compensated [3]. Nevertheless, this configuration might generate a higher detent force, so other solutions must be also combined if a good overall performance is to be achieved [121].

Conventional methods for dealing with the cogging force of LMs are equally effective in LMs. Fractional-slot designs are a good solution to reduce the cogging force [80]. PM-arc adjustment, semi-closed slots and asymmetric PM arrangements [69] are also another option to reduce the cogging effect. The skew is another effective way to deal with the cogging force [68], [81], [123].

In the detent force optimisation, a periodic model can be used in FEM first [133]. In this way, there is no end effect, and the effectiveness of the selected cogging suppression solution can be evaluated. Then the real machine can be simulated, including the end force mitigation technique. The difference between the no-load forces of the real machine and the periodic machine is the end effect force.

In the case of the modular, segmented, or partitioned-primary configurations, it may be very difficult to obtain the same results from the simulations in experimental machines, due to the manufacturing tolerances. It was stated in [5] that some thermally conductive epoxies such as Epoxies 50-3185 NC can be used to hold the pieces in place. However, if some pieces are slightly displaced, additional thrust ripple components might appear in the experimental machines [102], which are very hard to predict.

C. POWER FACTOR

The low power factor is one of the main issues for LPPMs. So far, there are not many solutions that have been found to be effective in the literature. However, the usage of V-shaped IPMs [164], [168], [169], [172] is a good alternative. In this study, this solution has not been found in LFRPMs and LSFPMs but both of them could benefit of this configuration.

Another choice is the usage of a double-sided configuration with a series magnetic circuit [155], [170], [171]. As mentioned before, an impressive power factor of 0.945 has been reported in [171], but there are no experimental results that validate this value. By means of example, a double-mover C-Core LSFPM is shown in Fig. 18 with a series magnetic circuit. It is a known issue that C-Core LSFPMs suffer from low power factor [106], so the proposed topology can possibly improve the performance of conventional LSFPMs.

D. FAULT-TOLERANT CAPABILITY

Fault tolerance is achieved by reducing the ratio between the mutual inductance and the self inductance. This can be achieved with the adoption of fault tolerant teeth [132], [134]. The idea behind fault-tolerant teeth is that it serves as a return path for the flux generated by a phase. In this way, the different phases can share less flux, enhancing their electromagnetic isolation.

Modular configurations are an even better solution for improving the fault-tolerance of LMs [134], [163], [184]. What is interesting with this topology is that if the distance between the modules is increased, the decoupling between phases is increased. If there is a big enough margin from the machine size point of view, the designer has the flexibility of deciding which the adequate displacement is.

E. NORMAL FORCE

The high normal force is one of the main disadvantages of single-sided LMs [124]. Double-sided configurations can compensate the unbalanced normal force [92], [124]. However, if a series magnetic circuit is employed [124] the normal force fluctuates, so it still has to be taken into consideration when sizing the linear bearings. The other main solution for balancing the normal force is the adoption of a tubular topology [189]. However, as stated in [189], tubular machines shall be employed only in short-strokes, so that deformation of the long part is avoided.

VII. QUALITATIVE COMPARISON OF LINEAR PRIMARY PM MACHINES

In order to fulfil both cost and high energetic efficiency requirements, modern drive systems must adopt highly efficient actuators which can be reasonably cost effective in terms of the required materials and the manufacturing process. In this section, a qualitative comparison table is given. The table is based on the literature research. The table serves as a summary of the capabilities of LPPMs, to allow designers to select the ideal topology for a given list of requirements.

Thrust density, shear stress, thrust per PM volume, detent force, thrust ripple and PM immunity are discussed in this section. Typical values for the design parameters like the linear loading, current density, or magnet remanence are within the same range for all the types of machines, with of 20-35 kA/m, 3.5-7.5 A/mm^2, and 1.2-1.35 T respectively.

As discussed in the previous section, the power factor is very low for LVPMs, and although it has not been analysed as much for LFRPMs, the same performance could be deduced from their RM counterparts. No references to the power factor of doubly-salient machines have been found in the literature, so this characteristic is left out of the table. However, as a general reference, LVPMs show power factor values ranging from 0.3 to 0.6, and the range for LSFPMs in the literature is 0.7-0.85.

For LDSPMs, as mentioned before, there are not many mentions in the literature, but the machines that have been found can generate ~100 kN/m^3, with a shear stress range of 6.4-10.7 kN/m^2. Regarding PM usage, these machines generate 3.6-7 MN/m^3. The detent force and thrust ripple of these machines are also quite high, especially for the basic configuration, with 35-50 % detent force and 40-55 % thrust ripple. However, applying skew or a modular configuration this values can be reduced to 8.5-16.5 % and 12-15 %. As for PM immunity, LDSPMs are said to have an excellent demagnetisation withstand capability.

In case of LFRPMs, the thrust density range is much larger due to the partitioned-primary configuration [138]. This machine, with 560 kN/^{3} can generate much higher thrust force than the other configurations in the literature, generally ranging around 150-200 kN/m^3. The shear stress of LFRPMs is generally found to be around 7-8 kN/m^2, and the magnet usage is also quite good, with values of 5-8 MN/m^3. In this case, the thrust capability per PM volume of large slot-opening LFRPM machines is calculated to be of 11.5 MN/m^3 [141], only surpassed by the 19.6 MN/m^3 generated by the partitioned-primary LFRPM. Detent and thrust forces are generally lower than in the case of LDSPMs. In both cases, 5-10 % values are often found in the literature. The main drawback of LFRPMs comes when analysing their PM immunity, with an inherently low resistance against PM demagnetisation [137], [143].

The thrust density of LSFPMs has been found to range around 300-500 kN/m^3 depending on the selected structure. The shear stress usually ranges ~10-13 kN/m^2, and ripple factors lower than 5 % are rarely found in the literature, with a typical range of 8-15 %. Although the PM demagnetisation immunity is great for the LSFPMs, due to their problematic flux leakage, they generally produce ~2.5-4 MN/m^3 of PM volume. In these aspect, both E-core and C-Core machines can produce ~7 MN/m^3, thus considerably reducing the cost of the active part of the machine.

Finally, the shear stress that can be generated by vernier machines is off the charts. The most common values that have been found in the literature range between 20-50 kN/m^2, with reported values as high as 70 kN/m^2 [168]. Thrust density-wise, LVPMs are comparable to LSFPMs with 250-400 kN/m^3. The PM usage is also great with these machines, with commonly found values of 9-15 MN/m^3 of magnet volume. Another great advantage of LVPMs are the low values of detent force and thrust ripple that they normally exhibit. These can normally be found to be ~5 % for LVHM machines, or even lower for LPPMVMs. The main disadvantages of these machines are the low power factor and the weak PM immunity.

TABLE 1. Qualitative comparison of LPPMs.

	LDSPM	LFRPM	LSFPM	LVPM
Thrust Density	✓	✓✓	✓✓✓✓	✓✓✓✓
Shear Stress	✓✓	✓✓	✓✓✓	✓✓✓✓✓
Thrust per PM Volume	✓✓✓	✓✓✓	✓✓	✓✓✓✓✓
Detent & Thrust Ripple	✓	✓✓✓	✓✓	✓✓✓✓✓
PM Immunity	✓✓✓✓	✓	✓✓✓✓✓	✓
Control Typology	BLDC or BLAC	BLAC	BLAC	BLAC

TABLE 2. Main dimensions of the machines.

Parameter	Unit	LFRPM	LSFPM	LVHM	LPMSM
Active Length	mm	200			
Machine Depth	mm	100			
Total Height	mm	35			
Airgap	mm	0.4			
Nph	Turns	100			
Rated Linear Loading	kA/m	20			
Rated Speed	m/s	1			
PM Remanence	T	1.2			
PM Relative Permeability		1.034			
PM Volume	mm^3	10532	63340	12923	54649
Current Density	A/mm^2	6.5	3.5	7.5	3.5

VIII. PERFORMANCE EVALUATION OF DIFFERENT MACHINE TECHNOLOGIES

To this date, no paper has been published comparing the capabilities of LFRPMs, LSFPMs, and LVPMs. Based on Table 1, LDSPMs have been discarded, due to their relative low thrust density and high ripple.

The characteristics of the machines are often listed without any comparison between different technologies. Thus, in this section, in order to validate the relative comparison in Table 1, the three machines are sized and compared under fixed dimensions and linear loading. The current density has been used to adjust the losses of the primary PM machines to similar values. This way, the relative capabilities of the machines for this requirement can be evaluated, so that the optimal machine for such requirement is identified. Moreover, the machines are compared to a conventional surface PM machine. This last machine allows to identify the drawbacks that adopting a primary PM structure might create.

The results of the comparison have been obtained in 2D FEM. The selected machine configurations, viz. consequent-pole large slot-opening LFRPM, C-Core LSFPM, consequent-pole LVHM, and fractional-slot concentrated winding LPMSM, and their main dimensions are shown in Fig. 23 and Table 2 respectively. The dimensions only take into account the active part of the machine.

A. THRUST FORCE

Figure 24 shows the average thrust of the machines under different current values. The rated current is 6.67 A for all

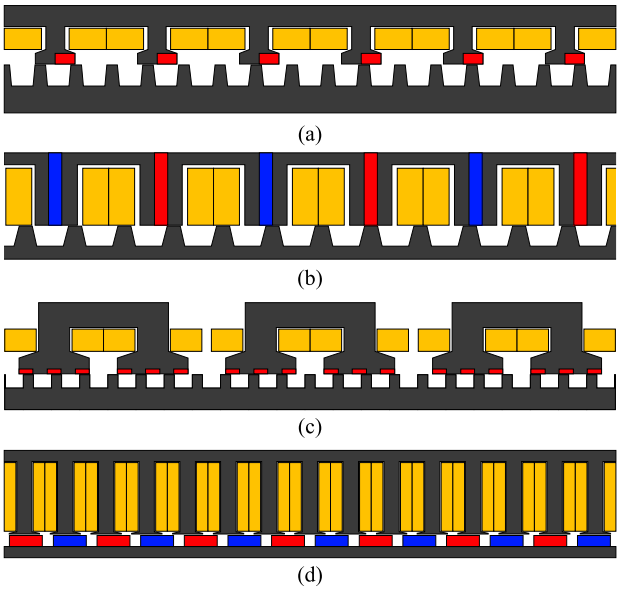

FIGURE 23. Compared machines. (a) LFRPM (b) LSFPM (c) LVHM and (d) LPMSM.

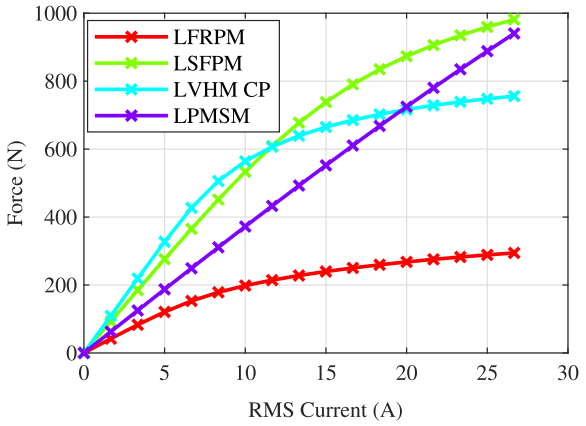

FIGURE 24. Average thrust force comparison.

machines. At rated current, the LVHM is the machine that generates the highest thrust force with 427.1 N, whereas the average thrusts of the LSFPM, LFRPM and LPMSM are 365.3 N, 153.2 N and 249.3 N respectively. Moreover, the rated thrust ripple of the LVHM is also the lowest between the three machines at 8.86 %. However, the overload capability of both the LSFPM and the LPMSM are superior to the rest. In case of the LPMSM, the average thrust curve is perfectly linear in the analysed range.

Due to the small airgap, all four machines exhibit high detent force values for their standards. That is why the thrust ripple values are also high, and reduce as the average thrust force is increased. However, in the case of the LPMSM and the LSFPM the detent force gets to 33.83 % and 50.5 % of the rated thrust, which are unacceptable most of the times.

B. POWER FACTOR

As stated in the literature search, the power factor of LFRPM machines has not been discussed yet. Figure 26 shows the

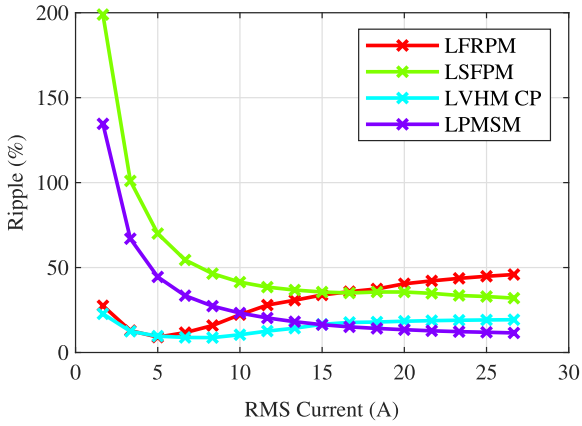

FIGURE 25. Thrust ripple comparison.

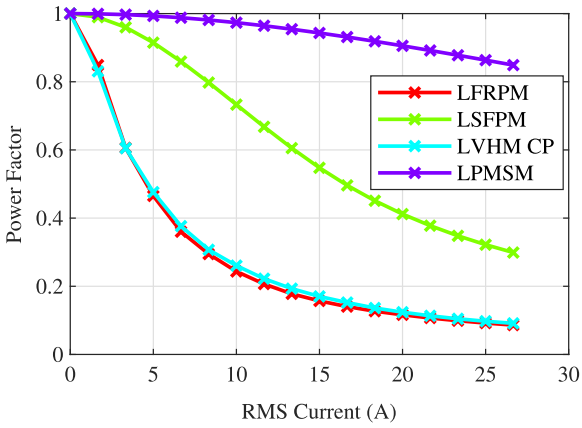

FIGURE 26. Power factor comparison.

evolution of the power factor of the four machines. Through the whole range, the power factors of both LFRPM and LVHM machines are almost identical, and much lower than the ones from the LSFPM and the conventional LPMSM. Thus, some especial configurations would be needed for these machines if the phase voltage and current were limited by an inverter.

In the case of the LSFPM, the power factor has an acceptable value around the nominal current value. However, the reduction of the power factor is much more severe than for the conventional LPMSM when operating at higher loads.

C. PM IMMUNITY

The evaluation of the PM immunity has been studied under two different conditions. First, the operating point of the PMs has been analysed in a no load simulation, to get the normal operating point of the magnets. Then, a faulty operation has been simulated, where a fully demagnetising current, i.e. in the negative d axis, of 6.67 A has been applied to every machine. Figure 27, Fig. 28, Fig. 29, and Fig. 30 show the results from the simulations. Notice that the scales of the figures are different. This was done in order to appreciate the change in the operating point with more detail.

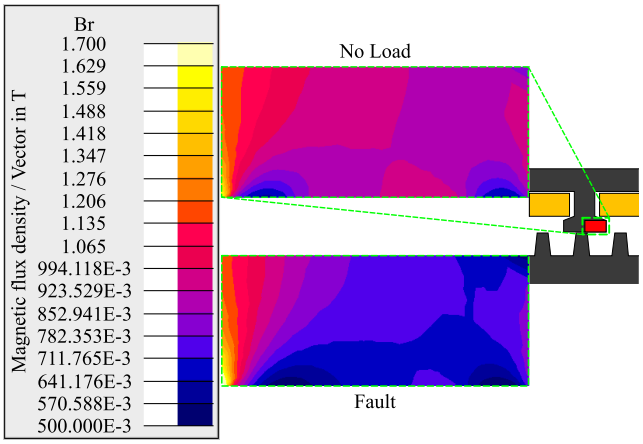

FIGURE 27. Operating point of the magnets of the LFRPM. No load (top) in fault condition (bottom).

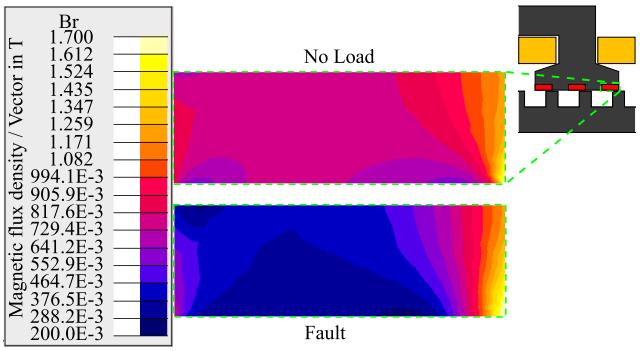

FIGURE 28. Operating point of the magnets of the LVHM. No load (top) in fault condition (bottom).

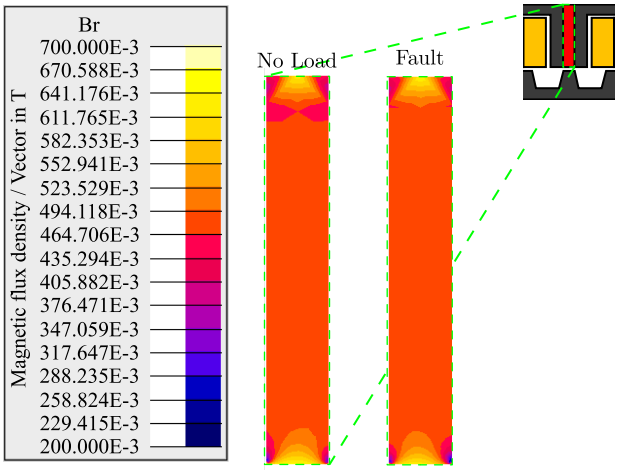

FIGURE 29. Operating point of the magnets of the LSFPM. No load (left) in fault condition (right).

Both LFRPM and LVHM machines are highly affected by the demagnetising current. The operating points of the magnets are reduced in around 0.21 T and 0.32 T respectively over the main area. In contrast, the LPMSM shows very little variation in the operating point of the magnet when the fault occurs. However, it is the LSFPM which exhibits the best PM immunity, because the operating point of the magnet shows no variation at all under the fault condition. Thus, it can be deduced that the best PM demagnetisation immunity is obtained by LSFPMs.

However, if the scales are analysed in detail, it can be clearly seen that the LSFPM shows some regions with a low operating point even in the no load simulation. Thus, there is a local demagnetisation risk even at normal operating conditions for these machines if this operating point is not taken into account when designing the machine. In addition, the operating point of the main flux generating area is also significantly lower for the PMs of the LSFPM in the no load simulation. This means that the LSFPM machine might require higher temperature grade magnets in order to avoid demagnetisation, which increases the cost of the PM material.

As a summary, all the results of the three machines are given in Table 3. The PM immunity field has been divided into two parts. The first field represents the immunity of the PMs to withstand demagnetising currents, and the second one refers to the PM remanence in normal operating point of the magnets.

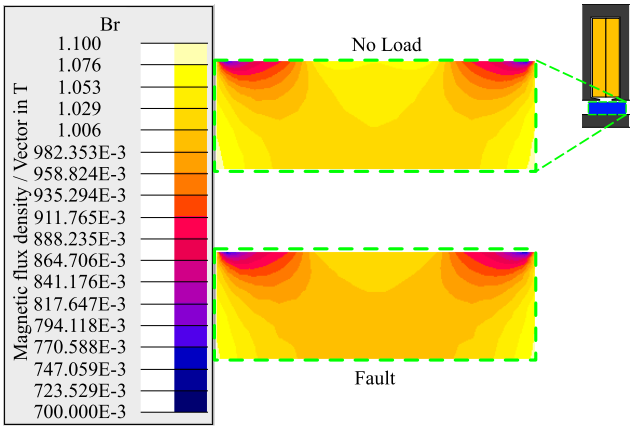

FIGURE 30. Operating point of the magnets of the LPMSM. No load (top) in fault condition (bottom).

TABLE 3. Performance comparison.

	Unit	LFRPM	LSFPM	LVHM	LPMSM
Thrust Density	kN/m^3	218.8	521.9	610.1	356.1
Shear Stress	kN/m^2	7.7	18.3	21.4	12.5
Thrust per PM Volume	MN/m^3	14.5	5.8	33.0	4.6
Detent Force	N-%	12.6-8.22	184.5-50.5	22.3-5.21	84.32 - 33.83
Thrust Ripple	%	11.7	54.5	8.9	33.4
PM Immunity (Fault)		✓✓	✓✓✓✓✓	✓	✓✓✓✓
PM Immunity (Normal)		✓✓✓✓	✓✓	✓✓✓✓	✓✓✓✓✓
Power Factor		0.36	0.86	0.38	0.99
Copper Loss	W	64.74	38.81	70.67	27.80
Iron Loss	W	23.62	46.75	22.3	19.22
Efficiency	%	63.41	81.02	82.12	84.13

D. RESULT DISCUSSION

First, it is important to mention that the aim of this comparison is not to obtain the globally optimised results for each type of machine. The comparison has been based on simple

configurations, in order to obtain typical capabilities of the machines.

Due to the small airgap to total height ratio, all the LPPMs exhibit slightly higher trust densities than the ones found in the literature. The low airgap length allows a larger flux linkage and thus a larger thrust capability for all machines.

For the same reason, the detent force is also high for all four machines. The increased no load flux attracts the machines with a stronger intensity. Thus, the amplitude of the ripple is enlarged.

The fault immunity of the machines also confirms what has been found in the literature, with high operating point variations for the magnets of the LFRPM and the LVHM.

The suspected low power factor has been confirmed for LFRPMs. In the analysed case, the power factor of the LFRPM is within the typical power factor range of LVPMs. This makes sense, because these machines are very similar constructively.

Under the same conditions, the thrust density and shear stress of the LFRPM are much lower than the ones of the other machines. So it can be concluded that the thrust capability of LFRPMs is significantly lower than the one of LSFPMs and LVHMs.

Even if the rated thrust density of the LVHM machine is the highest in between the analysed machines, in applications where the load is constantly changing, the overload capability must be taken into account when sizing the machine. For such applications, LVHM machines must be oversized. Thus, their thrust density has to be sacrificed. In this aspect, LSFPMs exhibit a combination high rated thrust density and good overload performance. However, it can be deduced from the results that the reduction of the overload capability is one of the main sacrifices that designers have to do when adopting the primary PM structure. As both the magnets and the PMs must be set in the primary side, there is less space for each component, and the magnetic circuit gets saturated at a lower loading value.

The thrust per PM volume confirms that the LSFPM needs much more costly active parts than the other LPPMs. Moreover, due to a naturally low operating point of the magnets, the temperature rating of the PMs in the LSFPM has to be higher than in the other LPPMs. This also leads to an increased cost of the active part. However, due to the poor power factor, both the LFRPM and the LVHM require costly inverters. This means that overall machine+inverter cost should be taken into account when selecting the ideal machine. If the conventional LPMSM is analysed, it can be seen that it demands an even higher PM volume than LSFPMs. Hence, not only can LPPMs be more cost effective than conventional LPMSMs in long stroke applications, but also in short stroke applications due to a lower PM volume requirement.

Regarding the thrust ripple, both the LFRPM and the LVHM exhibit acceptably low ripples, whereas the ripple of the LSFPM and the LPMSM are too high for most applications. This means that especial configurations must be adopted to deal with the detent force if LSFPMs or LPMSMs are selected.

If a robust operation is required, the LSFPMs are really good candidates, thanks to their outstanding withstanding of demagnetising currents. This feature can also allow to use these machines in strong field weakening conditions, without any risk of damaging the magnets.

IX. CONCLUSION

An exhaustive review of the current state of the linear machine technology was presented in this paper. First, the capabilities and operating principles of the different linear machine technologies were listed. Moreover, several configurations for enhancing their capabilities have also been presented. Thanks to the comprehensive review and analysis of the main machine technologies in the literature, the most promising LPPMs have been identified. By comparing these machines with a conventional LPMSM, the main sacrifices of adopting the primary PM structure have also been detected.

- The power factor of LPPMs is very low when compared to the conventional machine, especially in the case of the LFRPM and the LVPM.
- The overload capability of LPPMs is worse than the one of the conventional machine, due to the limitation in the available space.

As a direct comparison of the thrust capability and power factor between LSFPMs, LFRPMs, LVPMs and conventional LPMSMs has not been found in the literature, there are some interesting facts that can be concluded from the performance comparison. First, under the same restrictions, both the analysed LVHM and the LSFPM exhibit a higher rated thrust force density than the conventional LPMSM. Due to a strong flux focusing in LSFPMs, and the magnetic gearing of LVPMs, the thrust performance of the LPMSM can be enhanced. The overload capability of the LVHM has been found to be very limited when compared to the LSFPM. Such a poor overload capability may require an increased machine volume if the operating cycle of the machine contains frequently changing loads. In the case of LSFPMs, even if the PMs are immune to demagnetising currents, there is a local demagnetisation risk which must be assessed and its effect on their performance needs to be quantified.

The usage of series magnetic circuits could be a good solution for the enhancement of the power factor of LPPMs. In fact, partitioned-primaries inherently adopt a series magnetic circuit, but their effect on the power factor of linear machines has still not been analysed. Hence, series magnetic circuits with or without partitioned-primaries should be tested as a solution for enhancing the low power factor of these machines. In addition, the combination of a series magnetic circuit with hallbach arrays or V-shaped IPMs could also help in the improvement of the power factor while increasing the thrust capability of the LPPMs.

The partitioned-primary configuration is especially interesting for LVPMs, because it can be able to improve the thrust density while enhancing the power factor of the machines.

The thrust ripple reduction of ladder-slit secondary LIMs by adopting modular structures, or designs of mutually-coupled LSRMs for traction applications are also other fields that need to be assessed in future studies.

REFERENCES

[1] I. Boldea, *Linear Electric Machines, Drives, and MAGLEVs Handbook*, 1st ed. Boca Raton, FL, USA: CRC Press, 2013.

[2] R. Hellinger and P. Mnich, "Linear motor-powered transportation: History, present status, and future outlook," *Proc. IEEE*, vol. 97, no. 11, pp. 1892–1900, Nov. 2009.

[3] W. Hao and Y. Wang, "Thrust force ripple reduction of two C-core linear flux-switching permanent magnet machines of high thrust force capability," *Energies*, vol. 10, no. 10, p. 1608, Oct. 2017.

[4] I. Boldea, M. Pucci, and W. XU, "Design and control for linear machines, drives, and MAGLEVs—Part I," *IEEE Trans. Ind. Electron.*, vol. 65, no. 9, pp. 7423–7426, Sep. 2018.

[5] A. Gandhi and L. Parsa, "Thrust optimization of a flux-switching linear synchronous machine with yokeless translator," *IEEE Trans. Magn.*, vol. 49, no. 4, pp. 1436–1443, Apr. 2013.

[6] S. Yamamura, H. Ito, and Y. Ishulawa, "Theories of the linear, induction motor and compensated linear induction motor," *IEEE Trans. Power App. Syst.*, vol. PAS-91, no. 4, pp. 1700–1710, Jul. 1972.

[7] T. Yang, L. Zhou, and L. Li, "Finite element analysis of linear induction motor for transportation systems," in *Proc. IEEE Vehicle Power Propuls. Conf.*, Sep. 2008, pp. 1–4.

[8] N. Toro-García, Y. Garcés-Gómez, and F. Hoyos, "Discrete and continuous model of three-phase linear induction motors 'LIMs' considering attraction force," Considering Attraction Force," *Energies*, vol. 12, no. 4, p. 655, Feb. 2019.

[9] R.-J. Wai and C.-C. Chu, "Robust Petri fuzzy-neural-network control for linear induction motor drive," *IEEE Trans. Ind. Electron.*, vol. 54, no. 1, pp. 177–189, Feb. 2007.

[10] F. J. Lin, C. K. Chang, and P. K. Huang, "FPGA-based adaptive backstepping sliding-mode control for linear induction motor drive," *IEEE Trans. Power Electron.*, vol. 22, no. 4, pp. 1222–1231, Jul. 2007.

[11] A. H. Isfahani, B. M. Ebrahimi, and H. Lesani, "Design optimization of a low-speed single-sided linear induction motor for improved efficiency and power factor," *IEEE Trans. Magn.*, vol. 44, no. 2, pp. 266–272, Feb. 2008.

[12] B.-J. Lee, D.-H. Koo, and Y.-H. Cho, "Investigation of linear induction motor according to secondary conductor structure," *IEEE Trans. Magn.*, vol. 45, no. 6, pp. 2839–2842, Jun. 2009.

[13] A. Z. Bazghaleh, M. R. Naghashan, and M. R. Meshkatoddini, "Optimum design of single-sided linear induction motors for improved motor performance," *IEEE Trans. Magn.*, vol. 46, no. 11, pp. 3939–3947, Nov. 2010.

[14] B.-H. Lee, K.-S. Kim, J.-P. Hong, and J. H. Lee, "Optimum shape design of single-sided linear induction motors using response surface methodology and finite-element method," *IEEE Trans. Mag.*, vol. 47, no. 10, pp. 3657–3660, Oct. 2011.

[15] A. Shiri and A. Shoulaie, "Design optimization and analysis of single-sided linear induction motor, considering all phenomena," *IEEE Trans. Energy Convers.*, vol. 27, no. 2, pp. 516–525, Jun. 2012.

[16] S. E. Abdollahi, M. Mirzayee, and M. Mirsalim, "Design and analysis of a double-sided linear induction motor for transportation," *IEEE Trans. Magn.*, vol. 51, no. 7, pp. 1–7, Jul. 2015.

[17] A. A. Pourmoosa and M. Mirsalim, "Design optimization, prototyping, and performance evaluation of a low-speed linear induction motor with toroidal winding," *IEEE Trans. Energy Convers.*, vol. 30, no. 4, pp. 1546–1555, Dec. 2015.

[18] M. H. Ravanji and Z. Nasiri-Gheidari, "Design optimization of a ladder secondary single-sided linear induction motor for improved performance," *IEEE Trans. Energy Convers.*, vol. 30, no. 4, pp. 1595–1603, Dec. 2015.

[19] G. Lv, T. Zhou, D. Zeng, and Z. Liu, "Design of ladder-slit secondaries and performance improvement of linear induction motors for urban rail transit," *IEEE Trans. Ind. Electron.*, vol. 65, no. 2, pp. 1187–1195, Feb. 2018.

[20] J. Di, Y. Fan, Y. Liu, S. Liu, and Y. Zhu, "Variable pole pitch electromagnetic propulsion with ladder-slot-secondary double-sided linear induction motors," *Appl. Sci.*, vol. 7, no. 5, p. 481, 2017.

[21] G. Lv, T. Zhou, and D. Zeng, "Influence of the ladder-slit secondary on reducing the edge effect and transverse forces in the linear induction motor," *IEEE Trans. Ind. Electron.*, vol. 65, no. 9, pp. 7516–7525, Sep. 2018.

[22] R. Cao, Y. Jin, M. Lu, and Z. Zhang, "Quantitative comparison of linear flux-switching permanent magnet motor with linear induction motor for electromagnetic launch system," *IEEE Trans. Ind. Electron.*, vol. 65, no. 9, pp. 7569–7578, Sep. 2018.

[23] J. Zhan and Q. Lu, "Design optimization and performance investigation of novel linear induction motors with V-shaped ladder-slit secondary," *Int. J. Appl. Electromagn. Mech.*, vol. 58, no. 2, pp. 157–174, 2018.

[24] G. Lv, T. Zhou, D. Zeng, and Z. Liu, "Influence of secondary constructions on transverse forces of linear induction motors in curve rails for urban rail transit," *IEEE Trans. Ind. Electron.*, vol. 66, no. 6, pp. 4231–4239, Jun. 2019.

[25] J. Di, J. E. Fletcher, Y. Fan, Y. Liu, and Z. Sun, "Design and performance investigation of the double-sided linear induction motor with a ladder-slot secondary," *IEEE Trans. Energy Convers.*, vol. 34, no. 3, pp. 1603–1612, Sep. 2019.

[26] R. Cao, M. Lu, N. Jiang, and M. Cheng, "Comparison between linear induction motor and linear flux-switching permanent-magnet motor for railway transportation," *IEEE Trans. Ind. Electron.*, vol. 66, no. 12, pp. 9394–9405, Dec. 2019.

[27] J. Duncan, "Linear induction motor-equivalent-circuit model," *IEE Proc. B, Electr. Power Appl.*, vol. 130, no. 1, pp. 51–57, Jan. 1983.

[28] W. Xu, J. G. Zhu, Y. Zhang, Z. Li, Y. Li, Y. Wang, Y. Guo, and G. Li, "Equivalent circuits for single-sided linear induction motors," *IEEE Trans. Ind. Appl.*, vol. 46, no. 6, pp. 2410–2423, Dec. 2010.

[29] W. Xu, G. Sun, G. Wen, Z. Wu, and P. K. Chu, "Equivalent circuit derivation and performance analysis of a single-sided linear induction motor based on the winding function theory," *IEEE Trans. Veh. Technol.*, vol. 61, no. 4, pp. 1515–1525, May 2012.

[30] G. Lv, D. Zeng, and T. Zhou, "An advanced equivalent circuit model for linear induction motors," *IEEE Trans. Ind. Electron.*, vol. 65, no. 9, pp. 7495–7503, Sep. 2018.

[31] D. Zeng, G. Lv, T. Zhou, and M. Degano, "A complete equivalent circuit model for linear induction motor considering thrust, vertical and transversal forces," in *Proc. IEEE Int. Electr. Mach. Drives Conf. (IEMDC)*, May 2019, pp. 1766–1771.

[32] F.-J. Lin and R.-J. Wai, "Hybrid control using recurrent fuzzy neural network for linear induction motor servo drive," *IEEE Trans. Fuzzy Syst.*, vol. 9, no. 1, pp. 102–115, Feb. 2001.

[33] R.-J. Wai and W.-K. Liu, "Nonlinear control for linear induction motor servo drive," *IEEE Trans. Ind. Electron.*, vol. 50, no. 5, pp. 920–935, Oct. 2003.

[34] G. Kang and K. Nam, "Field-oriented control scheme for linear induction motor with the end effect," *IEE Proc. Electr. Power Appl.*, vol. 152, no. 6, p. 1565, 2005.

[35] B. Bessaih, A. Boucheta, I. K. Bousserhane, A. Hazzab, and P. Sicard, "Speed control of linear induction motor considering end-effects compensation using rotor time constant estimation," in *Proc. Int. Multi-Conf. Syst., Sygnals Devices*, Mar. 2012, pp. 1–7.

[36] A. Accetta, M. Pucci, A. Lidozzi, L. Solero, and F. Crescimbini, "Compensation of static end effects in linear induction motor drives by frequency-adaptive synchronous controllers," in *Proc. Int. Conf. Electr. Mach.*, 2014, pp. 716–723.

[37] F. Alonge, M. Cirrincione, M. Pucci, and A. Sferlazza, "Input-output feedback linearization control with on-line MRAS-based inductor resistance estimation of linear induction motors including the dynamic end effects," *IEEE Trans. Ind. Appl.*, vol. 52, no. 1, pp. 254–266, Jan. 2016.

[38] H. Karimi, S. Vaez-Zadeh, and F. R. Salmasi, "Combined vector and direct thrust control of linear induction motors with end effect compensation," *IEEE Trans. Energy Convers.*, vol. 31, no. 1, pp. 196–205, Mar. 2016.

[39] X. Song, D. Xu, W. Yang, Y. Xia, and B. Jiang, "Improved model-free adaptive sliding-mode-constrained control for linear induction motor considering end effects," *Math. Problems Eng.*, vol. 2018, May 2018, Art. no. 4341825, doi: 10.1155/2018/4341825.

[40] D. Hu, W. Xu, R. Dian, Y. Liu, and J. Zhu, "Loss minimization control of linear induction motor drive for linear metros," *IEEE Trans. Ind. Electron.*, vol. 65, no. 9, pp. 6870–6880, Sep. 2018.

[41] T. R. F. Neto and R. S. Pontes, "Design of a counterweight elevator prototype using a linear motor drive," in *Proc. IEEE Int. Electric Mach. Drives Conf. (IEMDC)*, vol. 1, pp. 376–380, May 2007.

[42] A. H. Selçuk and H. Kürüm, "Investigation of end effects in linear induction motors by using the finite-element method," *IEEE Trans. Magn.*, vol. 44, no. 7, pp. 1791–1795, Jul. 2008.
[43] N. S. Lobo, H. S. Lim, and R. Krishnan, "Comparison of linear switched reluctance machines for vertical propulsion application: Analysis, design, and experimental correlation," *IEEE Trans. Ind. Appl.*, vol. 44, no. 4, pp. 1134–1142, Jul./Aug. 2008.
[44] J. G. Amoros and P. A. Gascón, "Magnetic circuit analysis of a linear switched reluctance motor," in *Proc. 13th Eur. Conf. Power Electron. Appl. (EPE)*, 2009.
[45] J. Du, D. Liang L. Xu, and Q. Li, "Modeling of a linear switched reluctance machine and drive for wave energy conversion using matrix and tensor approach," *IEEE Trans. Magn.*, vol. 46, no. 6, pp. 1334–1337, Jun. 2010.
[46] J. G. Amoros and P. Andrada, "Sensitivity analysis of geometrical parameters on a double-sided linear switched reluctance motor," *IEEE Trans. Ind. Electron.*, vol. 57, no. 1, pp. 311–319, Jan. 2010.
[47] J. Garcia-Amorós, P. Andrada, and B. Blanqué, "Design Procedure for a Longitudinal Flux Flat Linear Switched Reluctance Motor," *Electric Power Compon. Syst.*, vol. 40, no. 2, pp. 161–178, Dec. 2011.
[48] X. Xue, K. W. E. Cheng, Z. Zhang, J. Lin, and N. Cheung, "A novel method to minimize force ripple of multimodular linear switched reluctance actuators/motors," *IEEE Trans. Mag.*, vol. 48, no. 11, pp. 3859–3862, Oct. 2012.
[49] J. F. Pan, N. C. Cheung, and Y. Zou, "An improved force distribution function for linear switched reluctance motor on force ripple minimization with nonlinear inductance modeling," *IEEE Trans. Magn.*, vol. 48, no. 11, pp. 3064–3067, Nov. 2012.
[50] X. Liang, G. Li, J. Ojeda, M. Gabsi, and Z. Ren, "Comparative study of classical and mutually coupled switched reluctance motors using multiphysics finite-element modeling," *IEEE Trans. Ind. Electron.*, vol. 61, no. 9, pp. 5066–5074, Sep. 2014.
[51] D. Wang, X. Wang, and C. Zhang, "Topology analysis and performance evaluation of a high thrust force density linear switched reluctance machine for low cost conveyor applications," in *Proc. 17th Int. Conf. Electr. Mach. Syst. (ICEMS)*, Oct. 2014, pp. 1283–1288.
[52] M. A. Kabir and I. Husain, "Mutually coupled switched reluctance machine (MCSRM) for electric and hybrid vehicles," in *Proc. IEEE Power Energy Soc. General Meeting*, Oct. 2014, pp. 1–5.
[53] D.-H. Wang, C.-L. Shao, X.-H. Wang, and X.-J. Chen, "Design and performance comparison of a bilateral yokeless linear switched reluctance machine for urban rail transit system," in *Proc. IEEE Vehicle Power Propuls. Conf. (VPPC)*, Oct. 2016, pp. 1–5.
[54] B. Ganji and M. H. Askari, "Analysis and modeling of different topologies for linear switched reluctance motor using finite element method," *Alexandria Eng. J.*, vol. 55, no. 3, pp. 2531–2538, 2016.
[55] G. J. Li, Z. Q. Zhu, X. Y. Ma, and G. W. Jewell, "Comparative study of torque production in conventional and mutually coupled SRMs using frozen permeability," *IEEE Trans. Mag.*, vol. 52, no. 6, pp. 1–9, Jun. 2016.
[56] H. Chen, R. Nie, and W. Yan, "A novel structure single-phase tubular switched reluctance linear motor," *IEEE Trans. Mag.*, vol. 53, no. 11, pp. 10–13, May 2017.
[57] D. Wang, X. Du, D. Zhang, and X. Wang, "Design, optimization, and prototyping of segmental-type linear switched-reluctance motor with a toroidally wound mover for vertical propulsion application," *IEEE Trans. Ind. Electron.*, vol. 65, no. 2, pp. 1865–1874, Aug. 2017.
[58] F. Hensley, A. W. Wong, W. C. Yu, and J. Ye, "Comparative analysis of conventional switched reluctance machines and mutually coupled switched reluctance machines," in *Proc. IEEE Transp. Electrific. Conf. Expo (ITEC)*, Jun. 2017, pp. 180–185.
[59] D. Wang, X. Wang, and X. Du, "Design and comparison of a high force density dual-side linear switched reluctance motor for long rail propulsion application with low cost," *IEEE Trans. Mag.*, vol. 53, no. 6, Jun. 2017, Art. no. 7207204.
[60] J. Du, D. Liang, and X. Liu, "Performance analysis of a mutually coupled linear switched reluctance machine for direct-drive wave energy conversions," *IEEE Trans. Mag.*, vol. 53, no. 9, pp. 1–10, Sep. 2017.
[61] D. Wang, D. Zhang, X. Du, and X. Wang, "Unitized design methodology of linear switched reluctance motor with segmental secondary for long rail propulsion application," *IEEE Trans. Ind. Electron.*, vol. 65, no. 12, pp. 9884–9894, Dec. 2018.
[62] J. F. Pan, W. Wang, B. Zhang, E. Cheng, J. Yuan, L. Qiu, and X. Wu, "Complimentary force allocation control for a dual-mover linear switched reluctance machine," *Energies*, vol. 11, no. 1, p. 23, 2018.
[63] J. Garcia-Amorós, "Linear hybrid reluctance motor with high density force," *Energies*, vol. 11, no. 10, p. 2805, 2018.
[64] D. Wang, D. Zhang, X. Du, and X. Wang, "Thermal identification, model, and experimental validation of a toroidally wound mover linear-switched reluctance machine," *IEEE Trans. Mag.*, vol. 54, no. 3, pp. 1–5, Nov. 2018.
[65] M. Vatani and M. Mirsalim, "Comprehensive research on a modular-stator linear switched reluctance motor with a toroidally wound mover for elevator applications," in *Proc. 10th Int. Power Electron., Drive Syst. Technol. Conf. (PEDSTC)*, Feb. 2019, pp. 61–66.
[66] P. Azer, B. Bilgin, and A. Emadi, "Mutually coupled switched reluctance motor: Fundamentals, control, modeling, state of the art review and future trends," *IEEE Access*, vol. 7, pp. 100099–100112, 2019.
[67] M. Inoue and K. Sato, "An approach to a suitable stator length for minimizing the detent force of permanent magnet linear synchronous motors," *IEEE Trans. Mag.*, vol. 36, no. 4, pp. 1886–1889, Jul. 2000.
[68] I.-S. Jung, J. Hur, and D.-S. Hyun, "Performance analysis of skewed PM linear synchronous motor according to various design parameters," *IEEE Trans. Magn.*, vol. 37, no. 5, pp. 3653–3657, Sep. 2001.
[69] K.-C. Lim, J.-K. Woo, G.-H. Kang, J.-P. Hong, and G.-T. Kim, "Detent force minimization techniques in permanent magnet linear synchronous motors," *IEEE Trans. Magn.*, vol. 38, no. 2, pp. 1157–1160, Mar. 2002.
[70] S. Vaez-Zadeh and A. H. Isfahani, "Multiobjective optimization of air-core linear permanent magnet synchronous motors for improved thrust and low magnet consumption," in *Proc. 8th Int. Conf. Electr. Mach. Syst. (ICEMS)*, Sep. 2005, vol. 1, no. 3, pp. 226–229.
[71] S. Vaez-Zadeh and A. H. Isfahani, "Multiobjective design optimization of air-core linear permanent-magnet synchronous motors for improved thrust and low magnet consumption," *IEEE Trans. Magn.*, vol. 42, no. 3, pp. 446–452, Mar. 2006.
[72] Y. W. Zhu and Y. H. Cho, "Thrust ripples suppression of permanent magnet linear synchronous motor," *IEEE Trans. Magn.*, vol. 43, no. 6, pp. 2537–2539, Jun. 2007.
[73] Y. Zhang, Y.-P. Chen, W. Ai, and Z.-D. Zhou, "Design strategy for detent force reduction of permanent magnet linear synchronous motor," *J. Shanghai Univ.*, vol. 12, no. 6, pp. 548–553, Dec. 2008.
[74] J. Wang, W. Wang, K. Atallah, and D. Howe, "Comparative studies of linear permanent magnet motor topologies for active vehicle suspension," in *Proc. IEEE Vehicle Power Propuls. Conf. (VPPC)*, Harbin, China, Sep. 2008, pp. 1–6.
[75] Y.-W. Zhu, D.-H. Koo, and Y.-H. Cho, "Detent force minimization of permanent magnet linear synchronous motor by means of two different methods," *IEEE Trans. Magn.*, vol. 44, no. 11, pp. 4345–4348, Nov. 2008.
[76] Z. Yu-wu, L. Sang-geon, and C. Yun-Hyun, "Topology structure selection of permanent magnet linear synchronous motor for ropeless elevator system," in *Proc. IEEE Int. Symp. Ind. Electron.*, Sep. 2010, pp. 1523–1528.
[77] B. Sheikh-Ghalavand, S. Vaez-Zadeh, and A. H. Isfahani, "An improved magnetic equivalent circuit model for iron-core linear permanent-magnet synchronous motors," *IEEE Trans. Magn.*, vol. 46, no. 1, pp. 112–120, Jan. 2010.
[78] Y. J. Kim and S. Y. Jung, "Minimization of cogging force in a stationary discontinuous armature linear permanent magnet motor at the outlet edge," *J. Magn.*, vol. 16, no. 3, pp. 288–293, 2011.
[79] J. J. Cai, J. Q. Ren, L. Cheng, and Y. Y. Ye, "Magnet skew technology investigation for the reduction of PMLSM thrust ripple," *Adv. Mater. Res.*, vols. 476–478, pp. 890–893, Feb. 2012.
[80] X. Wang, H. Feng, B. Xu, and X. Xu, "Research on permanent magnet linear synchronous motor for Rope-less hoist system," *J. Comput.*, vol. 7, no. 6, pp. 1361–1368, 2012.
[81] J.-J. Cai, Q. Lu, X. Huang, and Y. Yes, "Thrust ripple of a permanent magnet LSM with step skewed magnets," *IEEE Trans. Magn.*, vol. 48, no. 11, pp. 4666–4669, Nov. 2012.
[82] S.-G. Lee, S.-A. Kim, S. Saha, Y.-W. Zhu, and Y.-H. Cho, "Optimal structure design for minimizing detent force of PMLSM for a ropeless elevator," *IEEE Trans. Mag.*, vol. 50, no. 1, pp. 1–4, Jan. 2014.
[83] L. Huang, Y. Chen, H. Kong, Q. Lu, and Y. Ye, "Analysis of a permanent magnet linear synchronous motor with segmented armature for transportation system," in *Proc. 17th Int. Conf. Electr. Mach. Syst. (ICEMS)*, 2015, pp. 1791–1796.
[84] Y.-S. Kwon and W.-J. Kim, "Steady-state modeling and analysis of a double-sided interior permanent-magnet flat linear brushless motor with slot-phase shift and alternate teeth windings," *IEEE Trans. Mag.*, vol. 52, no. 11, pp. 1–11, Nov. 2016.

[85] Y.-S. Kwon and W.-J. Kim, "Detent-force minimization of double-sided interior permanent-magnet flat linear brushless motor," *IEEE Trans. Mag.*, vol. 52, no. 4, pp. 1–9, Apr. 2016.
[86] J. Song, F. Dong, J. Zhao, S. Lu, S. Dou, and H. Wang, "Optimal design of permanent magnet linear synchronous motors based on Taguchi method," *IET Electr. Power Appl.*, vol. 11, no. 1, pp. 41–48, Jan. 2017.
[87] A. So and W. Chan, "A study of linear PMSM driven ropeless elevators," *Building Services Eng. Res. Technol.*, vol. 40, no. 1, pp. 93–108, 2019.
[88] L. Zhang and K. Wang, "Design and analysis of PMLSM with SIN+3rd shaping mover," *Int. J. Comput. Math. Electr. Electron. Eng.*, vol. 37, no. 6, pp. 2158–2175, 2018.
[89] H. Wang, J. Li, R. Qu, J. Lai, H. Huang, and H. Liu, "Study on high efficiency permanent magnet linear synchronous motor for maglev," *IEEE Trans. Appl. Supercond.*, vol. 28, no. 3, pp. 1–5, Apr. 2018.
[90] X. Huang, T. Ji, L. Li, B. Zhou, Z. Zhang, D. Gerada, and C. Gerada, "Detent force, thrust, and normal force of the short-primary double-sided permanent magnet linear synchronous motor with slot-shift structure," *IEEE Trans. Energy Convers.*, vol. 34, no. 3, pp. 1411–1421, Sep. 2019.
[91] A. So and W. Chan, "Further study of linear PMSM driven ropeless lifts with consideration of imperfections by simulation," *Building Services Eng. Res. Technol.*, vol. 40, no. 6, pp. 682–697, 2019.
[92] X. Z. Huang, J. Li, C. Zhang, Z. Y. Qian, L. Y. Li, and D. Gerada, "Electromagnetic and thrust characteristics of double-sided permanent magnet linear synchronous motor adopting staggering primaries structure," *IEEE Trans. Ind. Electron.*, vol. 66, no. 6, pp. 4826–4836, Jun. 2019.
[93] X. Z. Huang, H. C. Yu, B. Zhou, L. Y. Li, D. Gerada, C. Gerada, and Z. Y. Qian, "Detent-force minimization of double-sided permanent magnet linear synchronous motor by shifting one of the primary components," *IEEE Trans. Ind. Electron.*, vol. 67, no. 1, pp. 180–191, Jan. 2020.
[94] C. Pollock and M. Wallace, "The flux switching motor, a DC motor without magnets or brushes," in *Proc. Conf. Rec. IEEE Ind. Appl. Conf. 34th IAS Annu. Meeting*, vol. 3, Oct. 1999, pp. 1980–1987.
[95] W. Hua, M. Cheng, Z. Q. Zhu, and D. Howe, "Design of flux-switching permanent magnet machine considering the limitation of inverter and flux-weakening capability," in *Proc. Conf. Rec. IAS Annu. Meeting (IEEE Ind. Appl. Soc.)*, vol. 5, Oct. 2006, pp. 2403–2410.
[96] J. Wang, W. Wang, R. Clark, K. Atallah, and D. Howe, "A tubular flux-switching permanent magnet machine," *J. Appl. Phys.*, vol. 103, no. 7, pp. 2006–2009, 2008.
[97] Z. Zhu, X. Chen, J. Chen, D. Howe, and J. Dai, "Novel linear flux-switching permanent magnet machines," in *Proc. Int. Conf. Electr. Mach. Syst.*, Wuhan, China, Oct. 2008, pp. 2948–2953.
[98] J. Wang, W. Wang, K. Atallah, and D. Howe, "Design considerations for tubular flux-switching permanent magnet machines," *IEEE Trans. Magn.*, vol. 44, no. 11, pp. 4026–4032, Nov. 2008.
[99] W. Hua, M. Cheng, Z. Q. Zhu, and D. Howe, "Analysis and optimization of back EMF waveform of a flux-switching permanent magnet motor," *IEEE Trans. Energy Convers.*, vol. 23, no. 3, pp. 727–733, Sep. 2008.
[100] Y. Pang, Z. Q. Zhu, D. Howe, S. Iwasaki, R. Deodhar, and A. Pride, "Investigation of iron loss in flux-switching PM machines," in *Proc. IET Conf. Publications*, no. 538, 2008, pp. 460–464.
[101] C. F. Wang, J. X. Shen, Y. Wang, L. L. Wang, and M. J. Jin, "A new method for reduction of detent force in permanent magnet flux-switching linear motors," *IEEE Trans. Magn.*, vol. 45, no. 6, pp. 2843–2846, Jun. 2009.
[102] Z. Q. Zhu, A. S. Thomas, J. T. Chen, and G. W. Jewell, "Cogging torque in flux-switching permanent magnet machines," *IEEE Trans. Magn.*, vol. 45, no. 10, pp. 4708–4711, Oct. 2009.
[103] M. J. Jin, C. F. Wang, J. X. Shen, and B. Xia, "A modular permanent-magnet flux-switching linear machine with fault-tolerant capability," *IEEE Trans. Magn.*, vol. 45, no. 8, pp. 3179–3186, Aug. 2009.
[104] Z. Q. Zhu and J. T. Chen, "Advanced flux-switching permanent magnet brushless machines," *IEEE Trans. Magn.*, vol. 46, no. 6, pp. 1447–1453, Jun. 2010.
[105] D. C. J. Krop, L. Encica, and E. Lomonova, "Analysis of a novel double sided flux switching linear motor topology," in *Proc. 19th Int. Conf. Electr. Mach. (ICEM)*, Sep. 2010, pp. 1–5.
[106] Z. Q. Zhu, "Switched flux permanent magnet machines—Innovation continues," in *Proc. Int. Conf. Electr. Mach. Syst. (ICEMS)*, 2011.
[107] W. Min, J. T. Chen, Z. Q. Zhu, Y. Zhu, M. Zhang, and G. H. Duan, "Optimization and comparison of novel E-core and C-core linear switched flux PM machines," *IEEE Trans. Mag.*, vol. 47, no. 8, pp. 2134–2141, Aug. 2011.
[108] C. F. Wang and J. X. Shen, "A method to segregate detent force components in permanent-magnet flux-switching linear machines," *IEEE Trans. Magn.*, vol. 48, no. 5, pp. 1948–1955, May 2012.
[109] R. Cao, M. Cheng, and W. Hua, "Investigation and general design principle of a new series of complementary and modular linear FSPM motors," *IEEE Trans. Ind. Electron.*, vol. 60, no. 12, pp. 5436–5446, Dec. 2013.
[110] Y. J. Zhou and Z. Q. Zhu, "Torque density and magnet usage efficiency enhancement of sandwiched switched flux permanent magnet machines using V-shaped magnets," *IEEE Trans. Magn.*, vol. 49, no. 7, pp. 3834–3837, Jul. 2013.
[111] J. Ji, S. Yan, W. Zhao, G. Liu, and X. Zhu, "Minimization of cogging force in a novel linear permanent-magnet motor for artificial hearts," *IEEE Trans. Magn.*, vol. 49, no. 7, pp. 3901–3904, Jul. 2013.
[112] Q. Lu, Y. Li, Y. Ye, J. Chen, and Z. Zhu, "A linear switched-flux PM machine with 9/10 primary/secondary pole number," in *Proc. 9th Int. Conf. Ecol. Vehicles Renew. Energies (EVER)*, Mar. 2014, pp. 1–7.
[113] R. Cao, M. Cheng, C. C. Mi, and W. Hua, "Influence of leading design parameters on the force performance of a complementary and modular linear flux-switching permanent-magnet motor," *IEEE Trans. Ind. Electron.*, vol. 61, no. 5, pp. 2165–2175, May 2014.
[114] F. Xiao, X. Liu, Y. Du, K. Shi, and P. Xu, "A C-core linear flux-switching permanent magnet machine with positive additional teeth," in *Proc. 17th Int. Conf. Elect. Mach. Syst. (ICEMS)*, Oct. 2014, pp. 1757–1761.
[115] Q. Lu, Y. Li, Y. Ye, J. Chen, and Z. Zhu, "Novel linear switched-flux PM machine with 9/10 primary/secondary pole number combination," *Int. J. Comput. Math. Electr. Electron. Eng.*, vol. 34, no. 6, pp. 1656–1672, Nov. 2015.
[116] Q. F. Lu, Y. X. Li, X. Y. Huang, and Y. Y. Ye, "Analysis of transverse-flux linear switched-flux permanent magnet machine," *IEEE Trans. Mag.*, vol. 51, no. 11, pp. 1–4, Nov. 2015.
[117] J. Liu, Y. Chen, Q. Lu, Y. Ye, and X. Huang, "Optimization and comparison of C-core and E-core linear switched-flux PM machines with odd primary poles," in *Proc. 18th Int. Conf. Electr. Mach. Syst. (ICEMS)*, Oct. 2015, pp. 254–259.
[118] B. Zhang, M. Cheng, S. Zhu, M. Zhang, W. Hua, and R. Cao, "Investigation of linear flux-switching permanent magnet machine for ropeless elevator," in *Proc. 19th Int. Conf. Electr. Mach. Syst. (ICEMS)*, Chiba, Japan, 2016, pp. 1–5.
[119] Q. Lu, Y. Yao, J. Shi, Y. Shen, X. Huang, and Y. Fang, "Design and performance investigation of novel linear switched flux PM machines," *IEEE Trans. Ind. Appl.*, vol. 53, no. 5, pp. 4590–4602, Sep. 2017.
[120] B. Zhang, M. Cheng, M. Zhang, W. Wang, Y. Jiang, and A. M. Topologies, "Comparison of modular linear flux-switching permanent magnet motors with different mover and stator pole pitch," in *Proc. 20th Int. Conf. Electr. Mach. Syst. (ICEMS)*, Sydney, NSW, Australia, 2017, pp. 1–5.
[121] Y. Du, G. Yang, L. Quan, X. Zhu, F. Xiao, and H. Wu, "Detent force reduction of a C-core linear flux-switching permanent magnet machine with multiple additional teeth," *Energies*, vol. 10, no. 3, p. 318, 2017.
[122] J. Liang, X. Ji, W. Gong, and W. Wang, "Design and analysis of a novel stator permanent magnet linear motor drive mechanical press," in *Proc. IEEE Int. Conf. Mechatronics Autom. (ICMA)*, Aug. 2018, pp. 1734–1738.
[123] W. Hao and Y. Wang, "Comparison of the stator step skewed structures for cogging force reduction of linear flux switching permanent magnet machines," *Energies*, vol. 11, no. 8, p. 2172, Aug. 2018.
[124] W. Hao and Y. Wang, "Analysis of double-sided sandwiched linear flux-switching permanent-magnet machines with staggered stator teeth for urban rail transit," *IET Elect. Syst. Transp.*, vol. 8, no. 3, pp. 175–181, Sep. 2018.
[125] R. Cao, Y. Jin, Z. Zhang, and M. Cheng, "A new double-sided linear flux-switching permanent magnet motor with yokeless mover for electromagnetic launch system," *IEEE Trans. Energy Convers.*, vol. 34, no. 2, pp. 680–690, Jun. 2019.
[126] Z. Zeng, J. Zhan, and Q. Lu, "Dynamic performance of dual-PM partitioned-primary hybrid-excited flux-switching linear machine," in *Proc. 13th Int. Conf. Electr. Mach. (ICEM)*, Sep. 2018, pp. 1492–1496.
[127] N. Ullah, A. Basit, F. Khan, W. Ullah, M. Shahzad, and A. Zahid, "Enhancing capabilities of double sided linear flux switching permanent magnet machines," *Energies*, vol. 11, no. 10, p. 2781, Oct. 2018.
[128] S. U. Chung, D. H. Kang, J. H. Chang, J. W. Kim, and J. Y. Lee, "New configuration of flux reversal linear synchronous motor," in *Proc. Int. Conf. Electr. Mach. Syst. (ICEMS)*, Seoul, South Korea, 2007, pp. 864–867.

[129] S.-U. Chung, H.-J. Lee, and S.-M. Hwang, "A novel design of linear synchronous motor using FRM topology," *IEEE Trans. Magn.*, vol. 44, no. 6, pp. 1514–1517, Jun. 2008.
[130] A. Gandhi, A. Mohammadpour, S. Sadeghi, and L. Parsa, "Doubled-sided FRLSM for long-stroke safety-critical applications," in *Proc. Ind. Electron. Conf. (IECON)*, 2011, pp. 4186–4191.
[131] L. Xu, W. X. Zhao, J. H. Ji, and G. H. Liu, "Design and analysis of a new linear fault-tolerant flux-reversal permanent-magnet machine," *Appl. Mech. Mater.*, vols. 416–417, pp. 3–8, Sep. 2013.
[132] W. Zhao, J. Ji, G. Liu, Y. Du, and M. Cheng, "Design and analysis of a new modular linear flux-reversal permanent-magnet motor," *IEEE Trans. Appl. Supercond.*, vol. 24, no. 3, pp. 1–5, Jun. 2014.
[133] A. L. Shuraiji, Z. Zhu, and Q. Lu, "A novel partitioned stator flux reversal permanent magnet linear machine," in *Proc. 10th Int. Conf. Ecol. Vehicles Renew. Energies (EVER)*, Mar. 2015, vol. 52, no. 1, pp. 1–8.
[134] L. Xu, G. Liu, W. Zhao, J. Ji, and Z. Ling, "Analysis of new modular linear flux reversal permanent magnet motors," *IEEE Trans. Mag.*, vol. 51, no. 11, pp. 1–4, Nov. 2015.
[135] J. Luo, B. Kou, Y. Zhou, and L. Zhang, "Analysis and design of an E-core transverse-flux flux-reversal linear motor," in *Proc. 19th Int. Conf. Electr. Mach. Syst. (ICEMS)*, Chiba, Japan, vol. 2, 2016, pp. 1–5.
[136] Z. Nasiri-Gheidari and F. Tootoonchian, "Electromagnetic design optimization of a modular linear flux-reversal motor," *Electr. Power Compon. Syst.*, vol. 44, no. 18, pp. 2112–2120, Nov. 2016.
[137] B. Kou, J. Luo, X. Yang, and L. Zhang, "Modeling and analysis of a novel transverse-flux flux-reversal linear motor for long-stroke application," *IEEE Trans Ind. Electron.*, vol. 63, no. 10, pp. 6238–6248, Oct. 2016.
[138] A. L. Shuraiji, Z. Q. Zhu, and Q. F. Lu, "A novel partitioned stator flux reversal permanent magnet linear machine," *IEEE Trans. Mag.*, vol. 52, no. 1, pp. 1–6, Jan. 2016.
[139] A. L. Shuraiji and Z. Q. Zhu, "Comparative study of two permanent magnet linear machines," in *Proc. 11th Int. Symp. Linear Drives for Ind. Appl. (LDIA)*, Sep. 2017, pp. 1–5.
[140] Z. Q. Zhu, A. L. Shuraiji, Q. F. Lu, and Y. Yao, "Experimental investigation of a partitioned stator flux reversal permanent magnet linear machine," in *Proc. 11th Int. Symp. Linear Drives Ind. Appl. (LDIA)*, Sep. 2017, pp. 1–5.
[141] C. Shi, R. Qu, Y. Gao, D. Li, and Y. Huo, "Design and optimization of a novel linear flux-reversal permanent magnet machines with large mover slot opening," in *Proc. IEEE Int. Magn. Conf. (INTERMAG)*, Apr. 2017, vol. 136, no. 1, p. 1.
[142] D. Dong, W. Huang, F. Bu, Q. Wang, W. Jiang, and X. Lin, "Modeling and static analysis of primary consequent-pole tubular transverse-flux flux-reversal linear machine," *Energies*, vol. 10, no. 10, p. 1479, Sep. 2017.
[143] S. Zhu, T. Cox, and C. Gerada, "Comparative study of novel tubular flux-reversal transverse flux permanent magnet linear machine," in *Proc. IEEE Energy Convers. Congr. Expo. (ECCE)*, Oct. 2017, pp. 4282–4287.
[144] D. Dong, W. Huang, F. Bu, and Q. Wang, "Analysis and optimization of a tubular permanent magnet linear motor using transverse-flux flux-reversal topology," in *Proc. 20th Int. Conf. Electr. Mach. Syst. (ICEMS)*, vol. 1, Aug. 2017, pp. 1–5.
[145] R. Cao, M. Cheng, C. Mi, W. Hua, and W. Zhao, "A linear doubly salient permanent-magnet motor with modular and complementary structure," *IEEE Trans. Magn.*, vol. 47, no. 12, pp. 4809–4821, Dec. 2011.
[146] R. Cao, M. Cheng, C. Mi, W. Hua, and W. Zhao, "A primary permanent-magnet linear motor for urban rail transit," *J. Int. Conf. Electr. Mach. Syst.*, vol. 1, no. 1, pp. 54–60, Mar. 2012.
[147] N. J. Baker, "Linear generators for direct drive marine renewable energy converters," Ph.D. dissertation, Dept. Eng. Comput. Sci., Durham Univ., Durham, U.K., 2003. Accessed: Feb. 26, 2019. [Online]. Available: http://etheses.dur.ac.uk/696/
[148] M. Mueller and N. Baker, "Modelling the performance of the vernier hybrid machine," *IEE Proc.-Electr. Power Appl.*, vol. 150, no. 2, pp. 139–145, 2003.
[149] M. A. Mueller and N. J. Baker, "Direct drive electrical power take-off for offshore marine energy converters," *Proc. Inst. Mech. Eng., A, J. Power Energy*, vol. 219, no. 3, pp. 223–234, May 2005.
[150] P. Brooking and M. Mueller, "Power conditioning of the output from a linear vernier hybrid permanent magnet generator for use in direct drive wave energy converters," *IEE Proc. Gener., Transmiss. Distrib.*, vol. 152, no. 5, p. 673, 2005.
[151] Y. Du, K. T. Chau, M. Cheng, Y. Fan, W. Zhao, and X. Li, "Theory and comparison of the linear stator permanent magnet vernier machine," in *Proc. Int. Conf. Electr. Mach. Syst.*, no. 1, Aug. 2011, pp. 1–4.
[152] Y. Du, K. T. Chau, M. Cheng, Y. Fan, Y. Wang, W. Hua, Z. Wang, "Design and analysis of linear stator permanent magnet vernier machines," *IEEE Trans. Magn.*, vol. 47, no. 10, pp. 4219–4222, Oct. 2011.
[153] J. Ji, J. Zhao, W. Zhao, Z. Fang, G. Liu, and Y. Du, "New high force density tubular permanent-magnet motor," *IEEE Trans. Appl. Supercond.*, vol. 24, no. 3, pp. 1–5, Jun. 2014.
[154] Y. Du, M. Cheng, K. T. Chau, X. Liu, F. Xiao, W. Zhao, K. Shi, and L. Mo, "Comparison of linear primary permanent magnet Vernier machine and linear Vernier hybrid machine," *IEEE Trans. Magn.*, vol. 50, no. 11, pp. 1–4, Nov. 2014.
[155] D. Li, R. Qu, and T. Lipo, "High-power-factor Vernier permanent-magnet machines," *IEEE Trans. Ind. Appl.*, vol. 50, no. 6, pp. 3664–3674, Nov./Dec. 2014.
[156] Y. Du, C. Zou, and X. Liu, "A double-sided linear primary permanent magnet vernier machine," *Sci. World J.*, vol. 2015, pp. 1–8, 2015.
[157] X. Liu, C. Zou, Y. Du, and F. Xiao, "A linear consequent pole stator permanent magnet vernier machine," in *Proc. 17th Int. Conf. Electr. Mach. Syst. (ICEMS)*, Oct. 2014, pp. 1753–1756.
[158] Y. Oner, Z. Q. Zhu, and W. Chu, "Comparative study of Vernier and interior PM machines for automotive application," in *Proc. IEEE Vehicle Power Propuls. Conf. (VPPC)*, Oct. 2016, pp. 1–6.
[159] D. Kameda, K. Hirata, and N. Niguchi, "Study of linear vernier motor for household automatic doors," in *Proc. 11th Int. Symp. Linear Drives Ind. Appl. (LDIA)*, Sep. 2017, pp. 1–4.
[160] F. Bian and W. Zhao, "A new dual stator linear permanent-magnet vernier machine with reduced copper loss," *AIP Adv.*, vol. 7, no. 5, p. 056679, May 2017.
[161] A. A. Almoraya, N. J. Baker, K. J. Smith, and M. A. Raihan, "Development of a double-sided consequent pole linear vernier hybrid permanent-magnet machine for wave energy converters," in *Proc. IEEE Int. Electr. Mach. Drives Conf. (IEMDC)*, no. 4, May 2017, pp. 1–7.
[162] A. A. Almoraya, N. J. Baker, K. J. Smith, and M. A. Raihan, "An investigation of a linear flux switching machine with tapered ferromagnetic poles," in *Proc. 20th Int. Conf. Electr. Mach. Syst. (ICEMS)*, 2017, pp. 1–5.
[163] T. Yao, W. Zhao, F. Bian, L. Chen, and X. Zhu, "Design and analysis of a novel modular-stator tubular permanent-magnet vernier motor," *IEEE Trans. Appl. Supercond.*, vol. 28, no. 3, pp. 1–5, Apr. 2018.
[164] C. Shi, R. Qu, Y. Gao, D. Li, L. Jing, and Y. Zhou, "Design and analysis of an interior permanent magnet linear vernier machine," *IEEE Trans. Mag.*, vol. 54, no. 11, pp. 1–5, Nov. 2018.
[165] F. Wu and A. M. El-Refaie, "Permanent magnet vernier machines: A review," in *Proc. 13th Int. Conf. Electr. Mach. (ICEM)*, Sep. 2018, pp. 372–378.
[166] X. Zhu, J. Ji, L. Xu, and M. Kang, "Design and analysis of dual-stator PM vernier linear machine with PMs surface-mounted on the mover," *IEEE Trans. Appl. Supercond.*, vol. 28, no. 3, pp. 1–5, Apr. 2018.
[167] H. Zhang, B. Kou, Z. Q. Zhu, R. Qu, J. Luo, and Y. Shao, "Thrust ripple analysis on Toroidal-winding linear permanent magnet vernier machine," *IEEE Trans. Ind. Electron.*, vol. 65, no. 12, pp. 9853–9862, Mar. 2018.
[168] A. A. Almoraya, N. J. Baker, K. Smith, and M. Raihan, "A new configuration of a consequent pole linear vernier hybrid machine with V-shape magnets," in *Proc. 13th Int. Conf. Electr. Mach. (ICEM)*, Sep. 2018, pp. 2002–2008.
[169] N. J. Baker, M. A. Raihan, A. A. Almoraya, J. W. Burchell, and M. A. Mueller, "Evaluating alternative linear vernier hybrid machine topologies for integration into wave energy converters," *IEEE Trans. Energy Convers.*, vol. 33, no. 4, pp. 2007–2017, Dec. 2018.
[170] W. Zhao, J. Zhu, J. Ji, and X. Zhu, "Improvement of power factor in a double-side linear flux-modulation permanent-magnet motor for long stroke applications," *IEEE Trans. Ind. Electron.*, vol. 66, no. 5, pp. 3391–3400, May 2019.
[171] W. Zhao, A. Ma, J. Ji, X. Chen, and T. Yao, "Multiobjective optimization of a double-side linear vernier PM motor using response surface method and differential evolution," *IEEE Trans. Ind. Electron.*, vol. 67, no. 1, pp. 80–90, Jan. 2020.
[172] A. A. Almoraya, N. J. Baker, K. J. Smith, and M. A. H. Raihan, "Design and analysis of a flux-concentrated linear vernier hybrid machine with consequent poles," *IEEE Trans. Ind. Appl.*, vol. 55, no. 5, pp. 4595–4604, Sep. 2019.
[173] A. Ma, W. Zhao, L. Xu, J. Ji, and F. Bian, "Influence of armature windings pole numbers on performances of linear permanent-magnet vernier machines," *IEEE Trans. Transport. Electrific.*, vol. 5, no. 2, pp. 385–394, Jun. 2019.

[174] M. A. H. Raihan, N. Baker, K. Smith, and A. Almoraya, "Linear consequent pole Halbach array flux reversal machine," *J. Eng.*, vol. 2019, no. 17, pp. 4560–4565, 2019.
[175] N. J. Baker, M. A. Raihan, and A. A. Almoraya, "A cylindrical linear permanent magnet vernier hybrid machine for wave energy," *IEEE Trans. Energy Convers.*, vol. 34, no. 2, pp. 691–700, Nov. 2019.
[176] F. Wu and A. M. El-Refaie, "Permanent magnet vernier machine: A review," *IET Electr. Power Appl.*, vol. 13, no. 2, pp. 127–137, Feb. 2019.
[177] N. Takahashi, S. Markon, and A. Onat, "Multi-objective optimization of the design of an elevator linear motor," in *Proc. IEEE Power Energy Soc. Gen. Meeting*, Jul. 2013, pp. 1–5.
[178] J. K. Xia, W. Y. Li, and L. Shen, "Skew and end-teeth optimization in reduce permanent-magnet linear synchronous motor normal force fluctuation," *Adv. Mater. Res.*, vols. 383–390, pp. 4853–4859, Nov. 2011.
[179] Q. F. Lu and W. H. Mei, "Recent development of linear machine topologies and applications," *CES Trans. Electr. Mach. Syst.*, vol. 2, no. 1, pp. 65–72, 2018.
[180] K. Chau, "Overview of electric vehicle machines—From tesla to tesla, and beyond," in *Proc. Int. Conf. Asian Union Magn. Soc. (ICAUMS)*, Aug. 2016, pp. 1–6.
[181] M. Cheng, W. Hua, J. Zhang, and W. Zhao, "Overview of stator-permanent magnet brushless machines," *IEEE Trans. Ind. Electron.*, vol. 58, no. 11, pp. 5087–5101, Nov. 2011.
[182] L. Ciacci, I. Vassura, Z. Cao, G. Liu, and F. Passarini, "Recovering the 'new twin': Analysis of secondary neodymium sources and recycling potentials in Europe," *Resour., Conservation Recycling*, vol. 142, no. Nov. 2018, pp. 143–152, 2019.
[183] D. G. Dorrell, I. Chindurza, and F. Butt, "Operation, theory and comparison of the flux reversal machine—Is it a viable proposition?" in *Proc. Int. Conf. Power Electron. Drive Syst.*, vol. 1, 2003, pp. 253–258.
[184] R. Cao, M. Cheng, C. Mi, W. Hua, X. Wang, and W. Zhao, "Modeling of a complementary and modular linear flux-switching permanent magnet motor for urban rail transit applications," *IEEE Trans. Energy Convers.*, vol. 27, no. 2, pp. 489–497, Jun. 2012.
[185] Z. Q. Zhu, "Overview of novel magnetically geared machines with partitioned stators," *IET Electr. Power Appl.*, vol. 12, no. 5, pp. 595–604, May 2018.
[186] J. Jimenez, "Diseño de motores lineales Síncronos miniaturizados para el accionamiento de puertas automáticas," Ph.D. dissertation, 2013.
[187] J. B. Wang and D. Howe, "Tubular modular permanent-magnet machines equipped with quasi-Halbach magnetized magnets—Part I: Magnetic field distribution, EMF, and thrust force," *IEEE Trans. Mag.*, vol. 41, no. 9, pp. 2470–2478, Sep. 2005.
[188] J. Faiz and A. Nematsaberi, "Linear permanent magnet generator concepts for direct-drive wave energy converters: A comprehensive review," in *Proc. 12th IEEE Conf. Ind. Electron. Appl. (ICIEA)*, Feb. 2018, pp. 618–623.
[189] I. Boldea, "Linear electromagnetic actuators and their control: A review," *EPE J. Eur. Power Electron. Drives J.)*, vol. 14, no. 1, pp. 43–50, 2003.

IMANOL EGUREN was born in Anoeta, Basque Country, Spain, in 1993. He received the B.S. degree in electronics engineering from Mondragon Unibertsitatea, Arrasate, Spain, in 2015, where he is currently pursuing the Ph.D. degree.

His current research interest includes design, control, and optimisation of linear machines.

GAIZKA ALMANDOZ (M'04) was born in Arantza, Spain. He received the B.Sc. and Ph.D. degrees in electrical engineering from Mondragon Unibertsitatea, Mondragon, Spain, in 2003 and 2008, respectively.

Since 2003, he has been with the Electronics and Computing Department, Faculty of Engineering, Mondragon Unibertsitatea, where he is currently an Associate Professor. His current research interest includes electrical machine design, modeling, and control. He has participated in various research projects in the fields of wind energy systems, elevator drive, and railway traction.

ARITZ EGEA received the degree in electrical engineering from the University of Mondragon, Mondragon, Spain, in 2009, and the Ph.D. degree in electrical engineering, in 2012.

He is currently an Associate Professor with the Faculty of Engineering, Mondragon Unibertsitatea. His current research interests include electrical machine design and control and electromagnetic actuators.

GAIZKA UGALDE (M'07) received the B.Eng. and Ph.D. degrees in electrical engineering from Mondragon Unibertsitatea, Mondragón, Spain, in 2006 and 2009, respectively.

Since 2009, he has been with the Department of Electronics, Faculty of Engineering, Mondragon Unibertsitatea, where he is currently an Associate Professor. His current research interest includes permanent-magnet machine design, modeling, and control. He has participated in various research projects in the fields of renewable energy and people transportation systems.

ANA JULIA ESCALADA was born in Pamplona, Spain, in April 1977. She received the B.S. degree in electronic engineering from the University of the Basque Country, Bilbao, Spain, in 2001, the B.Sc. degree in physics from the University of Cantabria, Santander, Spain, in 2003, and the Ph.D. degree in automatic and industrial electronic engineering from the University of Mondragón, Mondragón, Spain, in 2007, in conjunction with the Power Electronics Department, Ikerlan Technological Research Center.

She is currently with the Electrical Drives Department, ORONA EIC, Hernani, Spain. Her research interest includes drives and electrical machines for people transportation systems.